Final Report: Contribution of Particle Emissions from a Cement-Related Facility to Outdoor Dust in Surrounding Community

Paul J. Lioy, PhD, Zhi-Hua (Tina) Fan, PhD, and Chang Ho Yu, PhD
UMDNJ-Robert Wood Johnson Medical School and
Environmental and Occupational Health Sciences Institute
170 Frelinghuysen Road
Piscataway, NJ 08854

Submitted to:
Dr. Alan Stern
NJDEP Division of Science and Research
401 East State Street, Floor 1
Trenton, NJ 08625

March 02, 2009

1. Summary

A facility that processes steel production slag into material for cement manufacture is located near the neighborhood of Waterfront South (WFS), Camden, New Jersey. The residents in the vicinity of the facility have had concerns about the impact of the fugitive particulate emissions from the material stored and/or used at the facility on the neighborhood as outdoor dust air pollution. To address their concern, this study collected deposited particles and surface dust samples near the facility and the raw material (RCM) from the pile of the dust outside of the facility, analyzed morphological characteristics and elemental concentrations in the samples, and assessed the contribution of particles emitted from the facility to the dust pollution in local community. Specifically, we

a) developed deposition samplers to collect outdoor dust;
b) conducted two field sampling studies to collect deposited dust samples from 10-12 locations within the radial distance of approximately 700 m northeastern bound of the facility for a duration of 21 and 31 days, respectively;
c) collected two surface dust samples from 15 locations in the areas surrounding the facility;
d) analyzed the elemental compositions (cement-enriched elements including Ca, Fe, Al and Mg) of the deposited dust and surface dust samples;
e) analyzed morphological characteristics of the deposited dusts in subset of the samples and the RCM acquired from the facility; and
f) estimated the contribution of the faciltiy facility to outdoor dust by 1) comparing the elemental concentrations measured in the RCM with the deposited particle and surface dust samples, 2) conducting a regression analysis of calcium concentration as a function of distance from the piles and comparing the estimate of the concentration of attributable calcium in the deposited dust to the concentration of calcium in the RCM material and 3) conducting a source-receptor model (CMB v. 8.2, US EPA) using the elemental composition data obtained from this study.

The detailed study approach, results and discussion are presented below.

2. Methods

2.1 Site selection for deposited and surface dust collection

The raw material is stored outside of the facility without a cover. The pile of the material is about 9 m high. The pile is known to be supplied with new material by a wheel loader one or two time per week. Since the prevailing wind directions are southwest or northwest in the Camden area, the fugitive emissions from the raw material pile can be transported to the WFS neighborhood, which is located ~200 m downwind (i.e. northeast) of the facility (Figure 1).

To determine the impact of fugitive emissions from the facility on the WFS, we decided to collect deposition particle and surface dust samples in different locations in WFS. Before dust sample collection, we made two trips to Camden for site selection. The ideal sites for sampling would be locations that are easily accessed by field technicians, protected from inclement weather, and secure. Based on the site visits, the most appropriate sampling sites for collecting

re-suspended dusts emitted from the facility were located between the outer fence of the facility to Jackson Street, South 8th Street, and Morgan Street. The area is bounded by Route 676, Jackson Street, and Chelton Avenue, i.e. the main residential area of WFS that is located close to the piles of the raw material. In addition, the dust contains a significant proportion of large size particles (> 10 μm in diameter). We estimated the traveling distance for the fugitive dust in the size of 10 – 2,000 μm by wind using Equation (1) (Hinds, 1999).

$$L_d = \frac{H * V_X}{V_{TS}} \qquad (1)$$

$$V_{TS} = 3 * 10^{-5} * d^2 \ for \ 1 < d < 100 \ \mu m$$

where, L_d is the particle traveling distance (m),
V_{TS} is a terminal settling velocity (m/sec),
H is a vertical height of the particle settling (m),
V_X is a horizontal wind speed (m/sec), and
d is an aerodynamic diameter (μm)

Two levels of vertical height were used for estimate, one was 4.5 m (assuming that the particle transported from the middle height of the pile to the deposition sampler which was placed on the ground) and one was 9.0 m (assuming that the particle transported from the top of the pile to the deposition sampler), respectively. The wind speed of 3.5 m/s (median value) from June and September, 2006, which was reported by the Philadelphia International Airport Weather Station, was used for estimation. The weather station is located 12 km west of the facility and networked under the National Climate Data Center. The terminal settling velocity (V_{TS}) was calculated (for particles 10 < d < 100 μm) or obtained (for particles 100 < d < 2,000 μm) from a Table in the book of Aerosol Technology (2nd Edition, p56) assuming the aerodynamic diameter with standard density (1.0 g/cm^3) at standard condition (20 °C and 760 mmHg) with a laminar air flow (Reynold's number <1.0). Particles smaller than 10 μm in diameter are expected to travel farther than larger particles before settling on the ground. The estimated travelling distance for those particles are not included in Table 1 because calculation of traveling distance by Equation 1.1 can have a large error for that size fraction (Hinds, 1999).

As shown in Table 1, most coarse particles emitted from the facility will settle on the ground in areas within 800 m distance away from the facility, i.e. the impact of the fugitive dust are expected to be the highest in the WFS neighborhood. Thus, a total of 12 and 10 sites were selected in WFS for the first and second field deposition samplings, respectively. A control site was located at Gloucester City Park. The park is located 2.2 km Southwest of the facility, i.e. upwind of the plant. The sampling sites used for the two deposition field sampling studies are presented in Figures 4 and 5, respectively.

2.2 Collection of deposition dust

Based on a recent dry deposition study, which used a cellulose filter (8×10 inches) to measure lead deposition rate in the atmosphere (Franssens et al., 2004), we developed a dry deposition sampler that is suitable for the collection of particles in our study. The schematic diagram of the sampler is illustrated in Figure 2. Since we planned to collect samples for duration of 3-4 weeks, the rain and wind and security were considered when designing the

sampler. The sampler is plastic with a funnel hood to protect the filter from rain during field sampling. The sampler is painted dark green or black to minimize attention. The sampler can house up to four co-located quartz fiber filters 37 mm in diameter (Pall Life Sciences, Ann Arbor, MI). During sampling, the samplers were placed in open spaces to collect particles. Examples are: balcony, terrace, porch of resident's house; or a tree, or fence/electric pole. A photo of a field deposition sampler placed at a resident's home is shown in Figure 3.

The first deposition field sampling covered the period from July 5 to 26, 2007. Four samplers, including the one at the control site, were lost during the 21-day of sampling period. The samplers at these sites were relatively more visible and accessible than other locations. During the second field sampling which was conducted from August 17 to September 17, 2007, the samplers were placed at less visible locations. All samplers were recovered after the 31-day sampling period.

2.3 Collection of the surface dust

Based on previous experiences for undisturbed attic dust study (Ilacqua et al., 2003) and lead carpet dust intervention study (Yu et al., 2006), we decided to collect dust samples from flat surfaces using a wipe sampling method. The moistened wipe sample, Cliniguard Dry Washcloths, with size of 13×17.5 cm^2 (TENA, Waukegan, WI) were used in the study. Our previous studies showed that the moistened wipe could collect sufficient mass of dust for analysis on any flat surface reliably (Ilacqua et al., 2003; Yu et al., 2006).

Surfaces selected for sampling were tops of air conditioners, outdoor ledges/sills, and electrical boxes that are located close to the piles of raw material at the facility. These surfaces are better protected from the scavenging by the wind, but can be influenced by fugitive emissions. Also, they are flat and can be easily sampled by the wipe sampler. A visual inspection of a selected designated surface was completed prior to wipe sampling. Two wipe samples were collected from each 15 different sampling locations, and a total of 30 wipes were collected. The surface dust sampling locations are presented in Figure 5. It is worth to note that the particles deposited on surfaces with electrostatic force could be higher than those without electrical charges (Fews et al., 1999; Jeffers, 2006).

2.4 Collection of the raw material from the facility

The large pile of raw material (RCM) placed outside of the facility was considered to be the most important source of fugitive dust in the area. Thus, the bulk samples of raw material were collected from three upper locations where we could approach (~ 6 m high) of the pile. Each sample was collected from the top layer of each sampling location with a wide-mouth bottle (~ 150 g for each sample), and the three samples were combined as one sample to minimize the variability in the bulk material. Only one RCM sample was collected given our limited access to the facility. The RCM sample was stored in a temperature-controlled (4±1 °C) cold room at EOHSI prior to analysis.

2.5 Sample analyses

Analysis of elemental concentrations

After obtaining the weight of the dust mass the deposited dust samples, surface dust samples and the raw material obtained from the piles at the facility were analyzed for elements by a VG Elemental Plasma Quad 3 (PQ3) inductively coupled plasma mass spectrometry (ICPMS) at EOHSI.

For elemental analysis, the dust samples were digested by the microwave oven-assisted digestion method with concentrated high purity nitric acid (EPA methods TO-3050a and 3052). The RCM was sieved and the particles <38 μm in diameter were used for analysis. The size selection for RCM was based on the considerations of particles that would possibly transport to the target areas (see Table 1). The sieved RCM particles below 38 μm in diameter were 0.06% (by weight) of the whole bulk RCM. After digestion, the extract was analyzed for element by ICPMS. The ICPMS analysis conditions were similar to EPA method 200.8.

Field and lab blanks were concurrently analyzed with the samples. Sample concentrations were field blank subtracted before data analysis.

Microscopic analyses

Five settled dust samples collected from the 2nd deposition sampling study and one sample of the RCM were analyzed for morphology, size distribution, and elemental composition by the MVA Scientific Consultants (Duluth, GA). The five settled dust deposition samples were selected from the locations nearest to the facility (Location 1, 2, 3, 4 and 8) (see Figure 4). The RCM was sieved and particles <38 μm were submitted for analysis. The particle size and elemental composition were obtained using a JEOL Model JSM-6500F field emission scanning electron microscope (SEM), operating in automated mode under the control of a Thermo Noran System SIX x-ray analysis system. The morphological examination was conducted by polarized light microscopy (PLM) analysis using an Olympus SZ-40 stereomicroscope at magnifications from 7 to 40X. The reports prepared by MVA can be found in Appendix II~IV.

2.6 Data analyses

Descriptive Statistics

First, descriptive statistics was conducted to summarize the dust mass, loading, and elemental concentrations for the samples collected. Sampling method precision was also examined by calculating the difference in dust mass collected by 1) the four filters placed in one sampler and 2) %Diff (percent difference) between the mass collected by two co-located deposition samplers.

Association of the mass and elemental concentrations with the distance to the facility

Spearman correlation analysis was conducted to examine the association between the distance from each sampling site to the facility and the mass and element concentration in the dust collected at each site. The results were used to assess whether the dust mass would decrease as the distance to the facility increased.

Enrichment factors for elements

To explore the possibility of a contribution to dust deposition and surface dust by a possible source of raw material in the sampling area, a ratio for elements in given environmental sample to reference soil or rock was calculated for all elements that were quantified. This ratio, called the enrichment factor (EF), is an indicator for a source contributing to a background sample on the basis of elevated elemental concentrations (Adejumo et al., 1994). The enrichment factors defined in equation (2) were calculated using titanium (Ti) as a reference element. Titanium was chosen from a variety of elements analyzed in the study as a reference element based on the following requirements: 1) generally higher concentrations in reference rock or soil, 2) very low levels in pollution sources, 3) ease of determination by a number of analytical techniques, and 4) freedom from contamination during sampling.

$$EF = \frac{E_S / Ti_S}{E_r / Ti_r} \qquad (2)$$

where, EF is the calculated enrichment factor for a given element,

E_s is an elemental concentration or loading in the examined sample,

Ti_s is a titanium concentration or loading in the examined sample,

E_r is an elemental concentration in reference crustal rock, and

Ti_r is a reference titanium concentration in crustal rock (= 4,400 ppm)

In the above equation, the reference material concentration was obtained from Mason's crustal rock composition values (Rahn, 1976). An EF >5 indicates the presence of a source of the element in question that is causing it to be enriched in the sample material relative to the background soil (Adejumo et al., 1994).

Ca/Fe concentration ratios

The ratios of two elements, calcium and iron, were obtained to test the contribution of the raw material to outdoor dust. Calcium is a marker for cement-related activities and iron is a typical fingerprinting element for soil dust. Therefore, if the ratios are inversely proportional to proximity to the facility, the results indicate there are relative contributions of RCM to outdoor dust.

Chemical Mass Balance (CMB) model

A source apportionment was completed to estimate the contribution of particles emitted from the facility to the dust pollution in surrounding area. The Chemical Mass Balance (CMB) model (EPA version 8.2) was used for analysis. This source-receptor model involved the solution of linear equations that expresses each receptor chemical concentration as a linear sum of products of source fingerprint abundances and contributions (EPA, 2004). The CMB model requires detailed source profiles of each potential source located in the study area or profiles of similar sources in order to estimate the contribution of each source to the pollutant concentrations at each receptor. However, this study measured only the chemical composition of the raw material, one of the many potential sources for the outdoor dust in the study area. To utilize the CMB model, we employed source profiles from a well characterized published dataset, Portland Aerosol Characterization Study (PACS), which investigated the source-receptor relationship for $PM_{2.5}$, PM_{10} trace elements, ionic species and carbon in Portland, Oregon (Watson, 1979). The PACS source profiles included typical urban dust sources such as natural (e.g., marine aerosol and urban dust) and anthropogenic sources (e.g., automobile exhausts, oil combustions, and industrial emissions like paper mills and furnaces) in both fine-sized (<2.5 μm) and coarse-sized

(<10 μm) fractions. The concentrations of 19 elements, elemental and organic carbon, and sulfates/nitrates were quantified for all PACS sources. Also elemental concentrations in average rock and soil were added when building up the CMB source profile. The elemental abundances in reference rock (Mason 1966) and soil (Bowen 1966) were obtained from the report for chemical composition of the atmospheric aerosol study (Rahn, 1976).

Thus, the construction of CMB source profile was finalized with three sub-sets: 1) an elemental composition for the RCM sample analyzed in this study, 2) elemental concentrations in both reference rock and soil, and 3) six potential urban dust sources (marine aerosol, urban dust, automobile exhausts, residual oil combustion, aluminum production, and ferromanganese furnace). The contributions estimated from additional urban dust sources in the PACS study indicated that other potential dust sources, besides RCM and reference rock and soil, exist in the studied area and, as a whole, contribute to the increase of outdoor dust in the surrounding communities. However, each potential source can not be directly linked with the specific source, and detailed source specific information would be needed beyond the levels estimated by CMB model to characterize individual source contributions. Due to the high variability of elemental concentrations in surface dust samples (e.g., %Diff = 65 ± 37 % for 3 collocated duplicates), only dust deposition samples (N = 28) were used in the CMB model. The source elimination option was applied in running the CMB model to eliminate any negative source contribution estimate out of total nine source candidates. The contribution of RCM to outdoor dust was obtained from the estimated RCM contribution dividing by the sum of all source contribution estimates. The percentage calculated indicates the source contribution to each dust deposition sample examined by the CMB.

In the CMB model application default values were used to set up model options, and the performance of regression model was examined by investigating R^2, χ^2 and %Mass of the fitted models. The R-square (R^2) is the fraction of the variance in the measured concentrations that is explained by the variance in the calculated species concentrations. The reduced chi-square (χ^2) is the weighted sum of squares of the differences between the calculated and measured fitting species concentrations, and the percent mass (%Mass) is the percent ratio of the sum of the model-calculated source contribution estimates to the measured mass concentration (EPA, 2004). The CMB manual suggests that an $R^2 > 0.8$, $\chi^2 < 4.0$, and %Mass of 80 ~ 120 % provides an acceptable fit of the regression model (EPA, 2004). The CMB results showed 93 %, 89 %, and 64 % of the fitted receptors were found to be within the acceptable range of R^2, χ^2, and %Mass, respectively.

3 Results and Discussion

3.1 Particle mass and spatial distribution

The dust mass (mg) for the samples collected from the first and second deposition sampling studies is summarized in Tables 2 and 3, respectively. The mass ranged from 0.54 to 2.26 mg for a three-week sampling duration and 0.16 to 1.98 mg for a sampling duration of 31 days. The deposition sampling rate for the collected dust ranged from 2.39 to 10.01 μg/cm^2-day and between 0.48 ~ 5.94 μg/cm^2-day under the first and second samplings, respectively.

The deposition dust samples located close to the facility had higher dust mass. This inverse relationship between the dust mass collected and the distance from the facility was tested by a Spearman correlation. The analysis showed that the mass of dusts collected generally decreased with distances from the raw material pile (r_s = -0.7697; p = 0.0069), indicating the impact of the dust emitted from the facility to outdoor dust pollution.

Surface dust samples showed a larger variability in mass as well as loading (see Table 4). The collected mass and calculated loading for surface dust samples ranged from 1.71 to 227 mg and from 8.5 to 379.4 μg/cm^2, respectively. No spatial distribution of the surface dust mass was observed. This was probably because many factors can affect the retention of the dust on the flat surfaces, such as the previous dust deposition on the surface and scavenging of dust by rain and wind.

3.2 Particle size distribution

The particle size analysis (Table 5) revealed that the deposited dust was composed of mostly fine particles (< 2.5 μm), ranging from 78 to 88%. The fraction of coarse particles (2.5-10 μm) ranged from 11 to 19%. The similar size distribution was observed for the sample sieved from the RCM (with particle size of 38 μm and below in diameter). These results indicated that raw material dust contains significant numbers of inhalable particles, which can be of health concern. RCM contained 7.1% particles > 5 μm in diameter, relatively higher than the percentage of those particles found in the deposition samples (0.1, 3.7 and 4.3% for the 3 deposition samples respectively). This could be caused by the dry deposition collection substrate not holding all particles collected during the sampling duration due to the possible loss of particles by bouncing or blow-off by wind. This is especially the case for coarse particles, which can be scavenged by strong winds blowing over the filters in the field (Creighton et al., 1990). The actual mechanism is unknown, but it should be noted that large particles may be under-estimated by the dry deposition sampler. However, we should also note that larger particles normally will not deposit deep in the lung.

3.3 Elemental concentrations/loadings and spatial distribution

The elemental concentrations (ng/mg) for both deposited dust samples and RCM are presented in Tables 5 and 6 for 1st and 2nd deposition samplings, respectively. The elemental loadings (ng/cm^2) for surface dust samples are provided in Table 7. We found that Al (0.6 ~ 2.0 %), Ca (2.9 ~ 7.2 %), Fe (1.7 ~ 5.2 %), Mg (0.6 ~ 1.7 %), and Zn (0.1 ~ 2.0 %) were the most abundant elements in the dust deposition samples. Cu, Mn, Pb and Ti were the second abundant

elemental group in the deposited dusts, ranging mostly from 100 to 1,000 ng/mg in concentrations. The reported Cd, Cr, Si and V concentrations were primarily below 100 ng/mg. For surface dust samples, the loadings of each element were similar to the concentration order for the deposited dust samples. However, some wipes (for example Zn in both S007 and S020 and Cd in S020) had exceptionally higher levels compared to wipe samples collected at the other locations. An urban dust characterization study in Oslo, Norway found higher concentrations of Zn and Cd in the street dust collected from under the metal ledges and balconies of old buildings or around buildings undergoing renovations (Miguel et al., 1997). The elevated Cd and Zn concentrations may be linked with the corrosive action of urban rainwater (with pH of below 4.0 in many cases) by urban atmosphere, especially for coastal cities. The wipe sample (S020) was collected very close to the worn metal electric box mounted on a building wall, and another wipe sample (S007) was also collected on the top of painted electric box. Thus, the elevated metal loadings might be related with the metals deteriorated from the electric boxes by corrosive actions under urban atmosphere; however calcium loadings in two wipes were not significantly different from the loadings at other locations, suggesting the local source was limited to the increase of cadmium, iron and zinc in wiped samples.

The contribution of the facility's particle emissions to the dust deposition sample was examined by comparing the elemental concentrations/loadings in the dust samples and surface dust samples collected from each sampling locations to those derived from the RCM. Calcium concentrations measured in dust deposition samples are the most representative element showing a monotonic decrease with increase in the distance to the facility. With the inclusion of the background samples, (Gloucester City Park), there was a clear trend with $R^2 = 0.5412$ with a power function fit to the data (Figure 6(a)). To examine the calcium concentration influenced by the emission from the facility, the average %calcium concentration obtained from the background sites was subtracted from the %calcium concentration obtained at each residential sampling site to correct for background (i.e., non-facility) sources of calcium. The resulting background-corrected %calcium concentrations were plotted against the distances from each sampling site to the RCM pile located inside the facility. As shown in Figure 6(b), the trend of exponential decay in %calcium concentration with increasing distance from the facility remained, although the association was weaker (power function $R^2 = 0.3057$). The contributions (R) of the facility to the outdoor calcium concentration in the vicinity were estimated using the relationship established in Figure 6(b) and the calcium concentration of the RCM (i.e., 30.2%), as shown in equation (3). The estimated results are provided in Table 9. The calcium concentrations estimated here will be compared with the CMB estimates present in Section 3.5.

$$R = \frac{0.4318 \times D^{-1.0434}}{30.2} \qquad (3)$$

Where, R is the estimated calcium concentration (%)

D is the distance from each sampling site to the RCM pile located inside the facility (km)

The Spearman correlation showed that only calcium ($r_s = -0.7727$; $p = 0.0037$) had a statistically significant negative association between the concentration and the radial distance to the facility. This observation was consistent to the results reported in a previous atmospheric deposition study (Adejumo et al. 1994), i.e. calcium concentrations in deposited particles decreased exponentially along with the distance to three cement factories in Nigeria. Thus, our

results showed that the presence of raw material piled inside the facility contributed to the increase of calcium concentration in outdoor dust in the neighborhood around the facility.

However, the same relationship was not observed for the surface dust loadings ($p > 0.05$ for all elements). We suspected that the dust, which was re-suspended from the raw materials piles in the facility and settled on the open flat surface, were easily scavenged by rain and wind (Creighton et al., 1990), thus the dust mass collected by the surface wipe samples were not associated with the distance to the facility. Or, as will be discussed below, other sources contributed to the actual total dust loading.

3.4 RCM contributions to outdoor dust enrichment factors and Ca/Fe ratios

The enrichment factors (EF) for all elements analyzed in this study and Ca/Fe ratios are provided in Table 10. The EF of calcium was greater than 5 for the samples examined, indicating a significant contribution from the facility dust source, i.e. fugitive particulate emissions from RCM pile inside the facility associated with the sampling sites. Spearman correlation showed calcium's enrichment factors for deposited dusts were decreasing with the radial distances from the facility; however, the relationship was not significant ($r_s = -0.1273$; $p = 0.6932$). Similar results were also observed for surface dusts ($r_s = -0.3351$; $p = 0.1981$). Except for calcium, other elements did not show an inverse relationship between enrichment factors and radial distance from the facility. The Ca/Fe ratios were tested with the radial distances, too. A strong negative correlation was found for dust deposition samples ($r_s = -0.9000$; $p < 0.0001$; Spearman correlation), indicating the contribution of RCM to outdoor dust in the sampling area. However, the inverse relationship was not significant for surface dust samples ($r_s = -0.3410$; $p = 0.1900$). A previous study (Adejumo et al., 1994) reported significant contribution (approximately 21~30 %) of cement dust emitted from the cement production factories to neighborhood dust loadings located within 5 km in radial distance from the facilities.

The enrichment factors for Pb (ranged from 101 to 375 and from 68 to 2,860) and Zn (between 135 ~ 733 and 22 ~ 13,935) in both deposited dust and surface dust samples, respectively, were exceptionally higher than EFs for RCM (3.31 for Pb and 9.91 for Zn). These results suggested that there are local source(s) of Pb and Zn in these areas. Based on the local source information by the site visit, we found a metal treating facility, distant approximately 0.6 km from the study facility and providing services of abrasive blasting and painting processes, and an iron workshop located ~0.15 km from the Gloucester City Park, the background site, respectively. The radial distances from the nearest metal processing facility were obtained and the proximities were tested by a Spearman correlation for both Pb and Zn enrichment factors. The significant associations between EFs and radial distances were found for Pb ($r_s = -0.8061$; $p = 0.0026$) and Zn ($r_s = -0.7818$; $p = 0.0052$) in deposited dust samples; however, the associations were not significant for surface dusts ($p > 0.05$). This suggests the metal treating facility in Camden and an iron workshop in Gloucester City may attribute to the increase of lead and zinc concentrations in the ambient air locally; however, the proximity effect of these metal processing facilities was not conclusive for surface dusts, and other sources may be in the area including street dust for the lead.

3.5 CMB-model estimated RCM contributions to outdoor dust

The CMB model was completed for all dust deposition samples, and the source contributions (%) of RCM in the facility to outdoor deposited dusts are summarized in Table 11. The CMB modeling results for the deposition sample of D001-B collected from the closest site to the facility (within a radial distance < 0.2 km), are provided in Figure 7 as an example. The contributions of the RCM to outdoor dust at Site 1 (see Figure 4) and the control site, Gloucester City Park, which represented the closest and the farthest location to the facility, were estimated and are shown in Figure 8(a) and Figure 8(b), respectively.

The estimated contributions of the facility's dust to outdoor dust measured by deposition dust samplers ranged from 4.9 to 18.2 % (9.8 ± 3.7 %) and 5.6 to 21.8 % (13.1 ± 4.9 %) for 1st and 2nd deposition sampling studies, respectively. We observed that the RCM contributions to outdoor dusts were lower as the radial distances are farther from the facility (see Table 11). For example, the averaged RCM contributions were estimated to be 16.2 %, 8.5 %, and 8.9 % for dusts within the radial distance of 0-0.4 km, 0.4-0.66 km, and above 2.0 km from the facility, respectively. The CMB estimates agreed relatively well with the simple regression estimates which ranged from 2.4 to 8.1% (Table 9).

Two sensitivity factors that affect the CMB model estimable code (estimable vs. inestimable) are maximum source uncertainty (default = 20%) and maximum source projection (default of 95%) in CMB options window. We conducted the CMB modeling with the suggested default values, and in most cases, the sources tested were significantly estimable by the CMB model, except marine aerosols. Another significant factor for quantitative uncertainty in the model is the precision of the ambient and source profile data. We assumed an uncertainty approximately 10% for the mean of each element and put this value in input ambient and source data, if the uncertainty could not otherwise be estimated. For the study objectives, calcium in RCM was examined in detail to show the reliability of the source contribution estimates reported by the CMB model. The RCM was consistently selected as a significant source contributor (> 50% in Contribution by Species) and an influencing source (> 0.9 in MPIN Matrix) for all modeled dust deposition samples.

Considering the good agreement between the CMB model and the regression estimates as well as overall model performance diagnostics and additional model performance measures, the CMB model result was robust and reliable to estimate the RCM contributions to outdoor dust pollution in the neighborhood around the facility. The lack of emissions data for other sources in the studied area will provide some level of uncertainty in the results since the source emissions estimates used in the CMB modeling were from other areas. However, this technique has been applied widely in source apportionment analyses completed by the US EPA and other organizations (Chow et al., 1992; Watson et al., 1994; Schauer et al., 1996).

3.6 Contributions of the facility to outdoor dust estimated by ISCST3 model

The contributions from the stack and the entire site emissions of the facility (%) to total outdoor dust were estimated to provide the upper bound of the facility's contribution as well as the contribution (i.e., lower bound) by a dominant single stack in the facility. The estimation was based on 24-hour averaged TSP concentrations ($\mu g/m^3$) and conducted by the NJDEP using a US

EPA's Gaussian atmospheric dispersion model of ISCST3 (Industrial Source Complex Short Term) and size-dependent deposition velocities (mg/m^2-day). The detailed calculation procedures and results can be found in Appendix I in detail.

As discussed in section 3.5 (and Table 11) and also shown in Table 16 of Appendix I, the contribution of the raw material pile at the facility to outdoor dust in WFS ranged from 5.6% to 21.2% based on the CMB model estimation, and were between 2.4% and 8.1% based on the Ca concentrations of the deposition samples. In contrast, the estimated contributions from all site emissions, including operations of the plant, transportation of RCM by trucks, and stack emissions at the facility, using the ISCST3 model were 33.7%, 24.1%, and 18.3% for the distances of 200 m, 500 m, and 800 m, respectively, higher than the CMB as well as Ca-regression estimates. The higher contributions of the total site emissions estimated by the ISCST3 were reasonable, because in a number of cases these were worst case scenario estimates of emissions and the source strengths were of each stack and operations were considered constant each day. The contributions of a single stack emission (i.e., EP3 in Table 12) predicted by ISCST3 model were 3.6%, 4.0%, and 3.9% for the distances of 200 m, 500 m, and 800 m, respectively, only a small fraction of the total emissions from the facility. These results are reasonable because dust deposition is not expected to be significant in short distance given the height of the stack.

4 Conclusions

We conducted a study to investigate the contribution of fugitive particulate emissions from a facility in the neighborhood of WFS, Camden, NJ to outdoor dust from Jan 1, 2007 to June 30, 2008. One-month dust deposition samples and instantaneous area surface dusts were concurrently collected within the radial distance of approximately 700 m from the facility as well as outside the radial distance above 2.0 km upwind from the facility. The elemental concentrations and morphological characteristics showed that the re-suspended dusts from the raw material piles in the facility did have some impact on the residential areas surrounding the cement facility.

The contribution from the raw material piles to outdoor dust ranged from 4.9 % to 22 % calculated using the EPA approved source-receptor model (CMB v8.2). The results demonstrated the impact of particulate emissions from the piles on outdoor dust pollution in WFS area. The highest percent contributions were found to occur at locations between 0 and 0.4 km around the facility piles. Other sources contributed 75 % or more of the total outdoor dust pollution in the studied area, varying by locations.

For the site emissions including all sources in the facility, the contributions estimated using the results of the ISCST3 modeling were above 20% for the locations close to the facility (<500 m) and below 20% for the locations as far as 800 m distant from the facility. This was in a range similar to analyses reported that used the field data, but, as would be expected, the values were somewhat higher because of the conservative and worst case assumptions used to complete the ISCST3 modeling. Thus, the final conclusion is that the total plant contribution to outdoor dust is on average of <20% and probably on the order of 10%

References

Adejumo J. A., Obioh I. B., Ogunsola O.J., Akeredolu F. A., Olaniyi H. B., Asubiojo O. I., Oluwole A. F., Akanle O. A., and Spyrou N. M. The atmospheric deposition of major, minor and trace elements within and around three cement factories. Journal of Radioanalytical and Nuclear Chemistry (1994) Vol. 179, No. 2, 195-204.

Cheng M. D., Gao N., and Hopke P. K. Source apportionment study of nitrogen species measured in southern California in 1987. Journal of Environmental Engineering (1996), Vol. 122, 183-190.

Chow J. C., Watson J. G. Lowenthal D. H., Solomon P. A., Magliano K. L., Ziman S. D., and Richards L. W. PM_{10} source apportionment in California's San Joaquin Valley. Atmospheric Environment (1992) Vol. 26 (A), 3335-3354.

Creighton P. J., Lioy P. J., Haynie F. H., Lemmons T. J., Miller J. L., and Gerhart J. Soiling by atmospheric aerosols in an urban industrial area. Journal of the Air & Waste Management Association (1990) Vol. 40, No. 9, 1285-1289.

Dockery D. W., Pope C. A., Xu X., Spengler J. D., Ware J. H., Fay M. E., Ferris B. G., and Speizer F. E. An association between air pollution and mortality in six U.S. cities. New England Journal of Medicine (1993) Vol. 329, 1753-1759.

Edwards R. D., Yukrow E. J., and Lioy P. J. Seasonal deposition of housedusts onto household surfaces. The Science of the Total Environment (1998) Vol. 224, 69-80.

Ekinci E., Munlafalioglu I., Tiris M., and Pekin A. V. Characterization of cement plant emissions in Turkey. Water, Air, and Soil Pollution (1998) Vol. 106, 83-95.

Fews A. P., Henshaw D. L. Keitch P. A. Close J. J., and Wilding R. J. Increased exposure to pollutant aerosols under high voltage power lines. International Journal of Radiation Biology (1999) Vol. 75, 1505-1521.

Franssens M., Flament P., Deboudt K., Weis D., and Pedrix E. Evidence lead deposition at the urban scale using "short-lived" isotopic signatures of the source term (Pb-Zn refinery). Atmospheric Environment (2004) Vol. 38, 5157-5168.

Garland J. A. On the size dependence of particle deposition. Water, Air, and Soil Pollution: Focus (2001) Vol. 1, 323-331.

Hinds W. C. Aerosol Technology: properties, behavior, and measurement of airborne particles, Second Edition. (1999), John Wiley & Sons, Inc.

Ilacqua V., Freeman N. C. G., and Lioy P. J. The historical record of air pollution as defined by attic dust. Atmospheric Environment (2003) Vol. 37, 2379-2389.

Jeffers D. E. AC electric fields and particle deposition on a sphere. Radiation Protection Dosimetry (2006) Vol. 118, 56-60.

Lai A. C. K., Byrne M. A., and Goddard A. J. H. Experimental studies of the effect of rough surfaces and air speed on aerosol deposition in a test chamber. Aerosol Science and Technology (2002) Vol. 36, 973-982.

Lim J-H., Sabin L. D., Schiff K. C., and Stolzenbach K. D. Concentration, size distribution and dry deposition rate of particle-associated metals in the Los Angeles region. Atmospheric Environment 40 (2006) 7810-7823.

Lioy P. J., Freeman N. C. G., and Millette J. R. Dust: a metric for use in residential and building exposure assessment and source characterization. Environmental Health Perspectives (2001) Vol. 110, No. 10, 969-983.

Miguel E. D., Llamas J. F., Chacon E., Berg T., Larssen S., Royset O., and Vadset M. Orign and patterns of distribution of trace elements in street dust: unleaded petrol and urban lead. Atmospheric Environment (1997) Vol. 31, 2733-2740.

Mwaiselage J., Bratveit M., Moen B., and Yost M. Variability of dust exposure in a cement factory in Tanzania. Annals of Occupational Hygiene (2005) Vol. 49, No. 6, 511-519

Nazaroff W. W. Indoor particle dynamics. Indoor Air (2004) Vol. 14 (S. 7) 175-183.

Pumure I., Sithole S. D., and Kahwai S. G. T. Characterization of particulate matter emissions from the zimbabwe mining and smelting company (ZIMASCO) and Kwekwe division (Zimbabwe): a ferrochrome smelter. Environmental Monitoring and Assessment (2003) Vol. 87, 111-121.

Rahn K. A. The chemical composition of the atmospheric aerosol. Technical Report (1976), Graduate School of Oceanography, University of Rhode Island, Kingston, RI.

Schauer J. J., Rogge W. F., Hildemann L. M., Mazurek M. A., and Cass G. R. Source apportionment of airborne particulate matter using organic compounds as tracers. Atmospheric Environment (1996) Vol. 30, 3837-3855.

Thatcher T. L. and Layton D. W. Deposition, resuspension, and penetration of particles within a residence. Atmospheric Environment (1995) Vol. 29, No. 13, 1487-1497.

US EPA. EPA-CMB8.2 Users Manual. EPA-452/R-04-011, US Environmental Protection Agency, December 2004.

Wesely M. L. and Hicks B. B. A review of the current status of knowledge on dry deposition. Atmospheric Environment (2000) Vol. 34, 2261-2282.

Watson J. G. Chemical element balance receptor model methodology for assessing the sources of fine and total particulate matter in Portland, Oregon. Ph. D. Dissertation (1979), Oregon Graduate Center, Beaverton, OR.

Watson J. G., Chow J. C. Lu Z., Fujita E. M. Lowenthal D. H., and Lawson D. R. Chemical mass balance source apportionment of PM_{10} during the Southern California Air Quality Study. Aerosol Science and Technology (1994) Vol. 21, 1-36.

Yu C. H., Yiin L. M., and Lioy P. J. The bioaccessibility of lead (Pb) from vacuumed house dust in urban residences. Risk Analysis (2006) Vol. 26, No. 1, 125-134.

Appendices

I. Estimation of deposition flux and contributions to outdoor dust around the facility in WFS.

II. MVA report for microscopical analysis of particles on filters: D001-A, D005-A.

III. MNA report for microscopical analysis of particles on filters: D003-B, D018-C, D017-D.

IV. MVA report for microscopical analysis of RCM <38μm.

Table 1. The traveling distance for different size particles that may be emitted from the raw material pile at the median wind speed (3.5 m/s)[a] in the WFS neighborhood (Hinds, 1999).

Particle diameter (μm)	Settling velocity (cm/sec)	Particle travelling distance (m) for a settling height of 4.5 m[b]	Particle travelling distance (m) for a settling height of 9.0 m[c]
10	0.3	5,297	10,595
20	1.2	1,324	2,649
38	4.3	367	734
53	8.4	189	377
75	17	94	188
125	36	44	89
1000	386	4	8
2000	694	2	5

[a]The median wind speed during June and September, 2006 was obtained from the Philadelphia International Airport Weather Station located 12 km west of the facility.

[b]Assuming each sized aerodynamic particle traveled from the middle height of the raw material pile (4.5 m) to a deposition sampler on the ground level.

[c]Assuming each sized aerodynamic particle traveled from the top of the raw material pile (9 m) to a deposition sampler which was placed on the ground level.

Table 2. Summary of dust deposition samples collected for 3-week at Camden sampling sites (1st deposition dust field sampling).

Location	Sampler	Collected dust (N=4)		Co-located samplers		Comments
		Average (mg)	RSD (%)	Difference (mg)	%Diff[a]	
No. 1	001 002	1.523 1.560	5.5 5.0	0.037	2.4	Open space (fence)
No. 2	003 004	1.600 2.160	9.4 7.9	0.560	30	Open space (tree)
No. 3	005[b] 006[b]	NA	NA	NA	NA	Residence (front porch)
No. 4	007	1.422	4.5	NA	NA	Residence (front porch)
No. 5	010	0.912	9.5	NA	NA	Residence (front porch)
No. 6	011 012	1.103 1.093	13 11	0.010	0.9	Parking lot (tree)
No. 7	013 014	1.558 1.295	7.1 6.6	0.263	19	Open space (road sign)
No. 8	015[b] 016[b]	NA	NA	NA	NA	Residence (front porch)
No. 9	017 018	0.692 0.844	18 19	0.152	20	Parking lot (tree)
No. 10	019[b] 020[b]	NA	NA	NA	NA	Open space (sunshade)
No. 11	021[b] 022[b]	NA	NA	NA	NA	Control site (tree)
No. 12[c]	023	0.966	18	NA	NA	Residence (back yard)
				Ave. %Diff SD	14 12	

[a]Relative mean difference (%Diff) reported as percentage between two co-located samplers at the same location
[b]The deposition samplers were not recovered in the field

Table 3. Summary of dust deposition samples collected for 1-month at Camden sampling sites (2nd deposition dust field sampling).

Location	Sampler	Collected dust (N=4)		Co-located samplers		Comments
		Average (mg)	RSD (%)	Difference (mg)	%Diff[a]	
No. 1	001 002	1.730 1.477	14 18	0.253	16	Open space (tree)
No. 2	003 004	1.439 1.020	7.0 29	0.419	34	Open space (fence)
No. 3	005 006	1.202 1.230	14 7.2	0.029	2.3	Open space (tree)
No. 4[b]	007	0.796	9.4	NA	NA	Residence (front porch)
No. 5	008 009	1.586 1.614	8.0 8.7	0.028	1.7	Residence (back yard)
No. 6	010 011	1.042 1.082	9.6 10	0.040	3.7	Church (tree)
No. 7	012 013	0.990 1.154	4.2 1.7	0.164	15	Residence (back yard)
No. 8[b]	014	0.904	14	NA	NA	Residence (front porch)
No. 9	015 016	0.427 0.466	45 44	0.038	8.6	Control site (tree)
No. 10	019 020	0.550 0.560	15 9.3	0.010	1.8	Control site (tree)
				Ave. %Diff SD	10 10	

[a]Relative mean difference (%Diff) reported as percentage between two co-located samplers at the same location
[b]The sampling location deployed with two deposition samplers (covered vs. un-covered) only reported the result from the hooded type

Table 4. Summary of surface dust samples obtained at vicinities of the facility.

Sample	Collected weight (mg)	Loading ($\mu g/cm^2$)	Location	Sample	Collected weight (mg)	Loading ($\mu g/cm^2$)	Location
001-003	2.17±0.58[a]	NA	Field blank	021	31.54	70.7	Window sills
004-006	2.45±0.65[a]	NA	Lab blank	022	30.57	68.6	
007	80.99	38.7	Electrical box	023	29.49	52.0	Electrical box
008	19.12	42.0		024	35.37	41.8	
009	15.81	8.5	Outdoor table	025	21.03	38.4	Air conditioner
010	56.35	30.2		026	15.57	28.4	
011	44.77	73.0	Collecting box	027	7.17	10.6	Telephone booth
012	52.61	85.8		028	57.63	248.1	
013	15.38	47.3	Deserted boat	029	7.45	24.3	Electrical box
014	18.80	19.8		030	23.59	43.8	
015	158.89	259.1	Metal drum	031	12.56	23.7	Window sills
016	65.31	106.5	bin	032	39.79	97.3	
017	99.31	296.9	Outside air	033	22.13	12.7	Air conditioner
018	59.55	178.1	duct	034	3.61	14.4	
019	20.57	47.1	Electrical box	035	227.44	244.8	Vending
020	123.35	379.4		036	110.10	130.2	machine

[a]The number stands for average ± standard deviation from each three samples

Table 5. The result of particle size distribution (percent) for the RCM (RCM; sieved below 38-μm in diameter) and the deposited filters obtained from the facility**.**

Diameter Range (μm)	RCM	D001-A	D003-B	D005-A
0.5-1.0	56.0	36.5	4.4	26.8
1.0-2.5	30.4	51.6	79.6	58.4
2.5-5.0	6.5	8.3	15.9	10.7
5.0-7.5	2.4	1.5	0.0	2.1
7.5-10.0	1.6	0.7	0.1	0.7
>10.0	3.1	1.5	0.0	1.4
Particle Number Counted	950	1206	889	2000

Table 6. The result of elemental analyses[a] for deposited dust on filters by 1st deposition sampling around the facility in Camden, New Jersey**.**

L.	Sample	Mass (mg)	Distance[b] (km)	Al	Ca	Cd	Cr	Cu	Fe	Mg	Mn	Pb	Si	Ti	V	Zn
-	RCM	NA	0.00	18,991	301,988	DL[c]	34	58	7,801	14,595	877	10	17	1,006	10	148
1	D001A	1.401	0.23	12,133	60,585	3.1	56	166	22,270	12,114	662	294	254	679	51	2,413
	D001B	1.538		10,635	51,287	3.0	58	284	22,003	10,553	564	308	216	609	40	1,456
	D002A	1.560		13,697	56,875	5.8	84	192	26,635	11,809	653	355	159	874	52	2,562
2	D003A	1.683	0.37	10,172	42,163	4.3	92	394	28,568	10,598	511	582	141	627	48	2,699
	D004A	2.258		6,828	41,311	3.2	45	312	20,177	9,725	412	523	46	368	37	14,225
	D004B	2.238		6,253	37,033	3.2	48	279	19,964	8,671	355	458	124	323	39	20,080
4	D007A	1.441	0.36	8,854	35,961	3.2	74	260	26,232	9,049	422	420	132	545	33	1,820
5	D010A	1.037	0.50	6,378	29,449	6.5	50	185	16,816	5,871	296	282	215	410	29	1,439
6	D011A	0.971	0.66	7,675	37,672	15	94	329	34,480	8,198	444	501	199	471	41	3,265
	D012A	1.082		7,076	37,634	4.7	167	279	33,549	8,135	524	523	148	402	39	3,039
7	D013A	1.625	0.65	8,261	32,246	3.8	65	186	21,698	7,946	370	402	95	465	38	2,837
	D013B	1.648		9,538	37,573	5.8	70	344	26,893	9,305	478	600	88	502	49	8,011
	D014A	1.247		9,995	33,569	5.9	106	296	23,785	7,803	437	428	164	768	43	2,513
9	D017A	0.543	0.55	20,158	56,685	8.8	290	450	51,565	16,482	856	926	297	1,059	98	12,847
	D018A	1.034		16,194	41,344	5.4	336	261	41,248	11,922	662	618	88	1,070	71	4,504
12	D023A	0.751	0.45	14,684	61,438	11	177	335	43,196	14,876	787	730	151	780	66	4,421

[a]Concentration unit is ng/mg
[b]Distance was estimated from the sampling site to the RCM pile located inside the facility.
[c]DL means the concentration is below the method detection limit

Table 7. The result of elemental analyses[a] for deposited dust on filters by the 2nd deposition sampling around the facility in Camden, New Jersey.

L.	Sample	Mass (mg)	Distance[b] (km)	Al	Ca	Cd	Cr	Cu	Fe	Mg	Mn	Pb	Si	Ti	V	Zn
-	RCM	NA	0.00	18,991	301,988	DL[c]	34	58	7,801	14,595	877	10	17	1,006	10	148
1	D001-B	1.976	0.19	14,231	71,478	2.6	80	183	25,212	13,006	742	331	29	1,099	55	2,444
	D001-C	1.862		13,652	72,234	2.0	77	155	24,092	13,222	734	307	26	1,030	52	2,211
2	D003-C	1.512	0.29	10,918	51,138	2.8	97	172	24,034	10,918	589	347	26	877	53	2,411
	D003-D	1.482		9,761	46,221	2.4	172	174	24,777	10,363	582	661	34	760	53	2,383
3	D006-C	1.137	0.27	11,351	61,266	DL[c]	80	220	24,996	11,796	624	336	28	824	55	2,517
4	D007-D	0.800	0.35	11,910	67,100	3.7	104	349	38,475	14,795	660	615	51	826	65	2,990
5	D008-B	1.519	0.38	11,814	45,126	6.9	112	327	29,939	11,098	681	620	46	663	63	3,576
6	D011-B	1.151	0.61	12,598	45,770	11.0	710	251	51,364	14,189	813	550	47	497	65	5,797
7	D012-D	1.026	0.55	11,844	57,500	6.1	216	296	33,578	14,213	684	565	52	572	73	4,328
8	D014-C	0.872	0.45	11,954	50,493	4.9	106	307	29,661	16,773	621	359	69	690	138	5,105
9[d]	D016-C	0.608	2.38	7,284	33,202	5.7	124	186	20,249	8,404	392	330	26	427	40	2,118
10[d]	D020-C	0.594	2.20	11,121	47,845	5.0	140	238	28,185	17,027	522	265	70	808	123	4,848

[a]Concentration unit is ng/mg

[b]Distance was estimated from the sampling site to the RCM pile located inside the facility

[c]DL means the concentration is below the method detection limit

[d]Location 9 and 10 are representing typical elemental concentrations in deposited particles in the vicinity area of Camden, New Jersey.

Table 8. The result of elemental loadings[a] for surface dust wipes collected by the surface dust sampling around the cement facility in Camden, NJ.

L.	Sample	Mass (mg)	Area (cm^2)	Dist. (km)	Al	Ca	Cd	Cr	Cu	Fe	Mg	Mn	Pb	Sb	Si	V	Zn
1	S007	80.99	2,090	0.24	3,908	1,022	0.2	34	20	2,274	184	23	40	33.6	<0[c]	4.1	5,882
2	S009	15.81	1,867	0.24	361	361	0.3	1	3	561	94	7	5	0.5	1	1.1	26
3	S011	44.77	613	0.27	1,304	2,688	0.1	26	11	4,198	1,484	29	31	DL[b]	<0[c]	3.3	155
	S012	52.61	613		570	1,220	0.1	22	8	3,010	1,802	32	23	1.3	7	4.7	87
4	S013	15.38	325	0.29	1,137	1,130	DL[b]	14	9	2,725	2,234	21	32	DL[b]	38	4.9	51
	S014	18.80	948		<0[c]	203	0.4	2	2	586	124	6	6	1.6	<0[c]	0.8	10
5	S016	65.31	613	0.27	1,083	3,565	0.1	16	14	3,575	399	26	9	0.9	<0[c]	2.9	60
6	S017	99.31	334	0.31	2,499	23,251	0.5	22	32	12,275	2,602	113	80	DL[b]	<0[c]	8.6	716
7	S020	123.4	325	0.32	7,708	10,067	656.8	78	224	96,808	2,611	271	1,142	15.9	3	83.6	10,299
8	S021	31.54	446	0.34	1,398	4,255	0.3	23	26	10,452	872	71	53	0.7	<0[c]	7.4	95
9	S023	29.49	567	0.32	<0[c]	579	4.4	4	12	2,824	333	19	317	13.1	<0[c]	4.6	86
	S024	35.37	845		1,005	1,840	1.4	9	16	4,477	419	26	149	93.4	<0[c]	5.0	110
10	S025	21.03	548	0.50	1,302	2,021	0.5	8	16	4,109	616	37	44	1.9	<0[c]	5.0	100
11	S028	57.63	232	0.43	5,451	14,474	1.1	58	131	24,297	4,234	176	296	7.2	<0[c]	24.1	700
12	S030	23.59	539	0.43	1,386	2,547	0.3	23	24	5,731	806	45	44	2.4	<0[c]	6.4	258
13	S032	39.79	409	0.37	1,832	5,596	0.1	15	20	7,086	1,451	38	104	DL[b]	<0[c]	8.7	489
14[d]	S033	22.13	1,747	2.01	236	344	0.0	4	3	605	121	6	6	DL[b]	<0[c]	2.2	37
15[d]	S036	110.1	845	2.01	2,828	2,230	0.1	29	42	7,063	837	51	45	8.7	<0[c]	15.1	80

[a]Loading unit is ng/cm^2

[b]DL means the concentration is below the method detection limit

[c]<0 means negative value after blank subtraction

[d]Location 14 and 15 are at background site, Gloucester City Park

Table 9. The original calcium concentrations, the background-subtracted calcium concentrations, and the estimated contribution to the calcium concentration from the cement facility emission to the surrounding residential areas based on the second deposition sampling results.

Location	Distance (km)	Original %Ca concentration	Background-Subtracted %Ca concentration	Estimated Contribution
Cement Pile	0.00	30.2	NA	NA
1	0.19	7.19	3.13	8.09%
2	0.29	4.87	0.82	5.20%
3	0.27	6.13	2.07	5.61%
4	0.35	6.71	2.66	4.28%
5	0.38	4.51	0.46	3.92%
6	0.61	4.58	0.52	2.39%
7	0.55	5.75	1.70	2.67%
8	0.45	5.05	1.00	3.29%
9	2.38	3.32	NA	NA
10	2.20	4.78	NA	NA

Table 10. Enrichment factors and Ca/Fe ratios for the deposited dust, surface dust, and RCM samples.

Element	RCM	Deposited Dust				Surface Dust			
		Sampling Sites (< 0.66 km)		Background (> 2.0 km)		Sampling Sites (< 0.5 km)		Background (> 2.0 km)	
	Mean	Mean	Range	Mean	Range	Mean	Range	Mean	Range
Al	1.02	0.86	0.67 – 1.37	0.84	0.75 – 0.94	1.62	0.43 – 7.97	1.21	0.69 – 1.72
Ba	5.10	7.24	4.27 – 10.5	5.56	4.63 – 6.48	28.0	1.43 – 143	4.02	3.48 – 4.57
Ca	36.4	9.23	7.07 – 12.2	8.02	7.18 – 8.86	5.76	0.95 – 21.2	1.18	0.09 – 2.26
Co	0.17	2.71	1.00 – 6.32	2.73	2.57 – 2.89	4.76	2.35 – 25.3	2.37	1.83 – 2.91
Cr	1.47	12.3	3.21 – 62.9	7.19	6.74 – 7.63	13.5	4.29 – 56.6	11.6	8.82 – 14.3
Cu	4.63	26.5	12.0 – 41.4	29.6	23.6 – 35.5	27.3	4.79 – 62.0	26.2	14.7 – 37.6
Fe	0.68	3.86	2.02 – 9.09	3.43	3.07 – 3.78	8.30	1.66 – 29.5	4.94	2.88 – 7.00
Ga	4.43	4.22	2.28 – 7.43	4.62	3.86 – 5.38	29.1	2.08 – 145	4.96	3.82 – 6.09
Li	3.35	3.77	2.45 – 6.05	3.94	3.80 – 4.08	5.15	1.16 – 16.0	3.98	2.42 – 5.53
Mg	3.06	3.64	2.49 – 6.01	4.78	4.44 – 5.11	2.96	1.46 – 6.45	1.68	1.37 – 1.98
Mn	4.04	4.20	3.11 – 7.57	3.58	2.99 – 4.17	2.97	0.67 – 4.34	2.09	1.51 – 2.67
Ni	0.34	7.48	3.28 – 18.8	6.93	6.35 – 7.52	6.33	1.27 – 17.8	6.09	4.60 – 7.59
Pb	3.31	224	101 – 375	144	111 – 176	538	67.8 – 2,860	143	114 – 173
Rb	0.15	0.90	0.57 – 1.37	1.42	1.39 – 1.46	1.03	0.28 – 2.21	1.38	0.80 – 1.95
Si	0.00	0.00	NA	0.00	NA	0.00	NA	0.00	NA
Sr	6.87	2.80	2.10 – 3.70	2.30	1.83 – 2.77	1.68	0.27 – 3.79	0.87	0.84 – 0.90
Ti	1.00	1.00	NA	1.00	NA	1.00	NA	1.00	NA
V	0.34	2.66	1.63 – 4.29	5.74	4.97 – 6.51	3.37	1.10 – 9.43	4.70	3.85 – 5.54
Zn	9.25	287	135 – 733	421	377 – 465	1145	22.1 – 13,935	91.4	56.7 – 126
Ca/Fe	38.7	2.00	0.89 – 3.00	1.70	1.70 – 1.70	0.58	0.10 – 1.89	0.44	0.32 – 0.57

Table 11. The percent estimation of RCM contribution to outdoor dusts by using an EPA CMB model based on elemental concentration compositions of RCM and other potential dust sources.

Sampling	Sampling site (< 0.4 km)			Sampling Site (0.4-0.66 km)			Background Site (> 2.0 km)		
	N	Mean	Range	N	Mean	Range	N	Mean	Range
1st	7	12.2 %	8.8–18.2 %	9	7.9 %	4.9–11.8 %	NA	NA	NA
2nd	7	16.2 %	12.4–21.8 %	3	8.5 %	5.6–10.9 %	2	8.9 %	8.89– 8.94 %

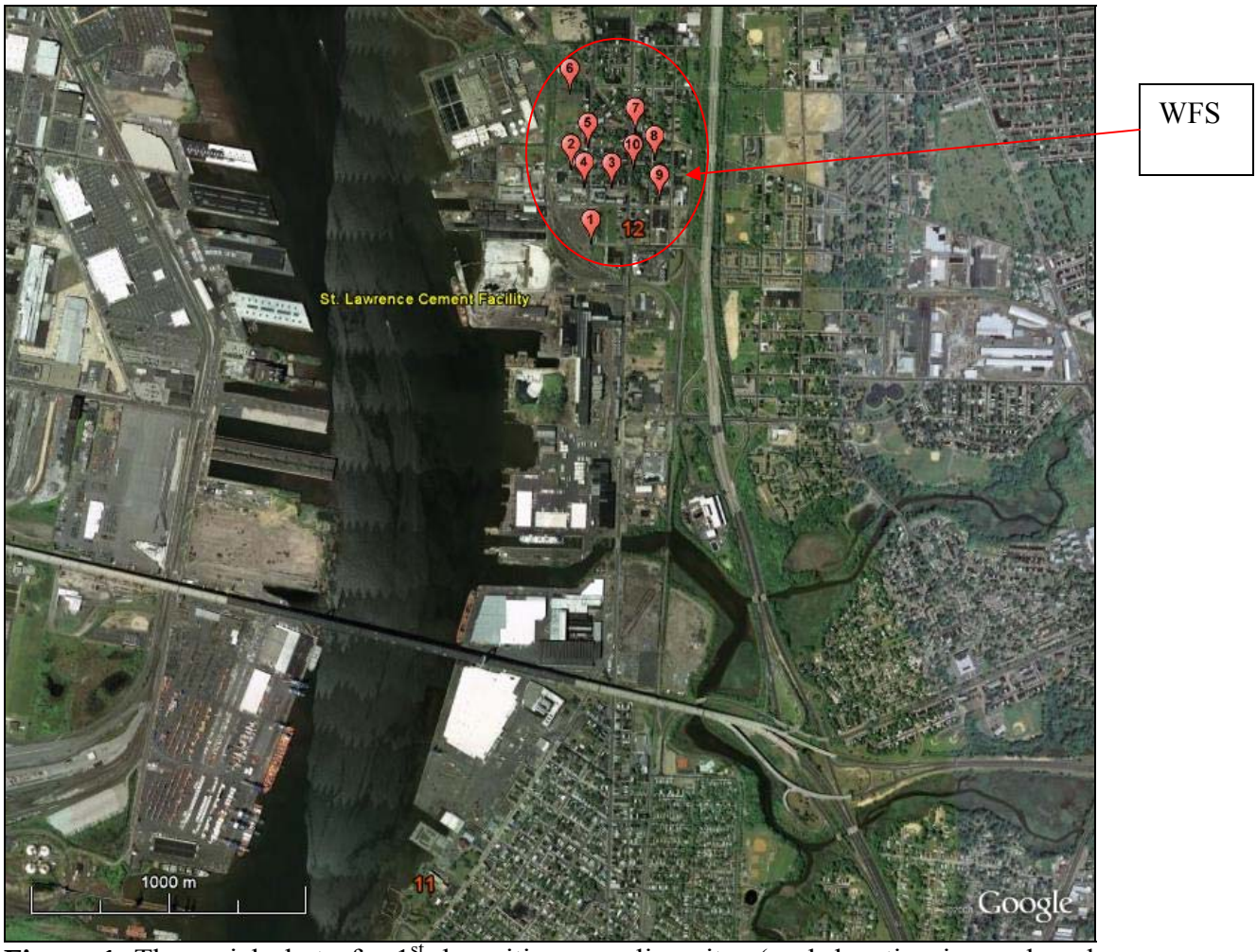

Figure 1. The aerial photo for 1st deposition sampling sites (each location is numbered 1~12 in the picture) to collect dusts in the neighborhood of WFS, Camden, New Jersey (obtained from Google Earth).

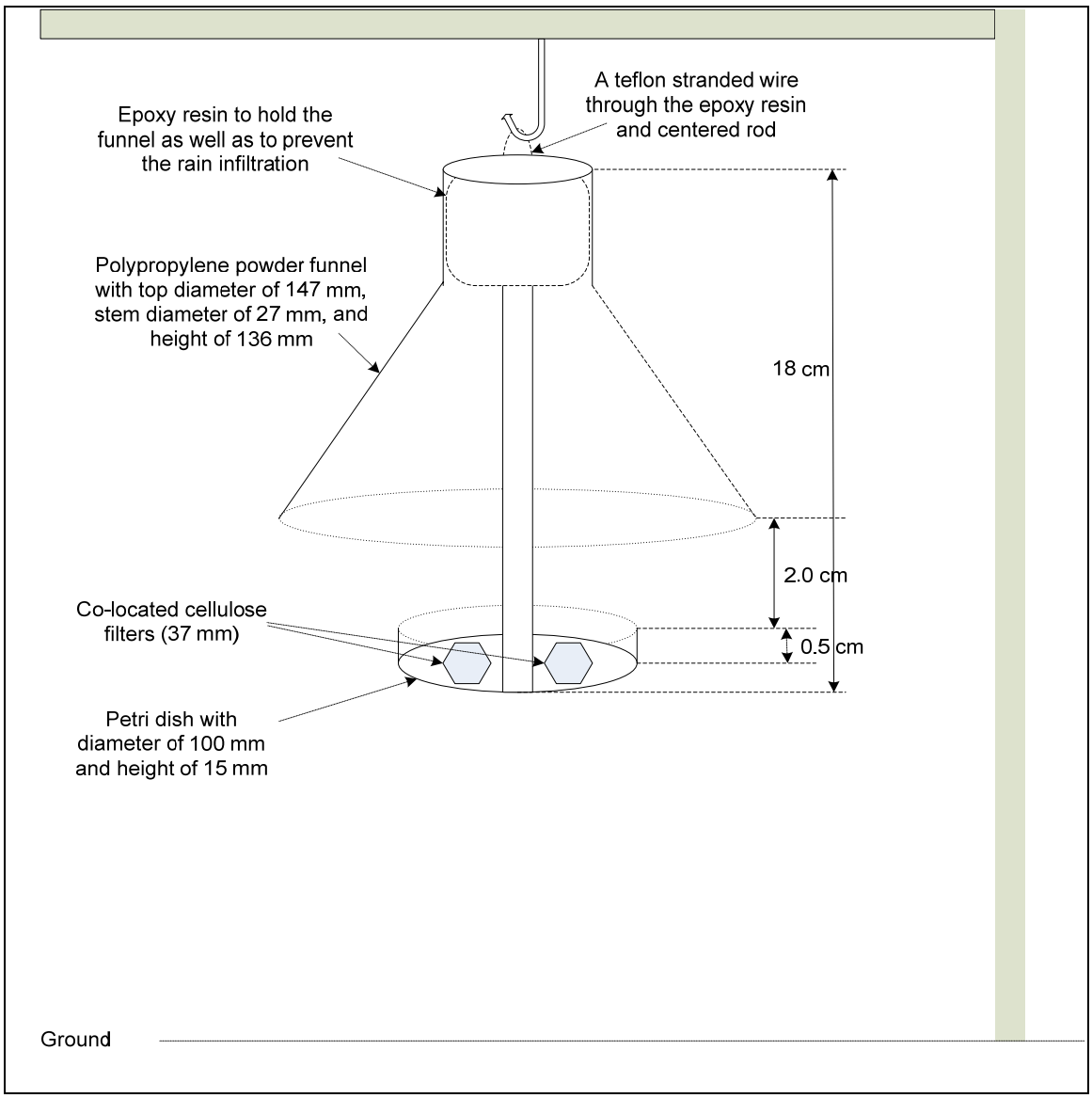

Figure 2. The drawing of deposition sample for the study.

Figure 3. A deposition sampler deployed in the field with (left) and without a cover (right).

Figure 4. The aerial photo for 2nd deposition sampling sites (each location is numbered 1~10 in the picture) to collect dusts in the neighborhood of WFS, Camden, New Jersey (obtained from Google Earth).

Figure 5. The aerial photo for surface sampling sites (each location is numbered 1~13 in the picture and background locations 14/15 are not displayed) to collect dusts in the neighborhood of WFS, Camden, New Jersey (obtained from Google Earth).

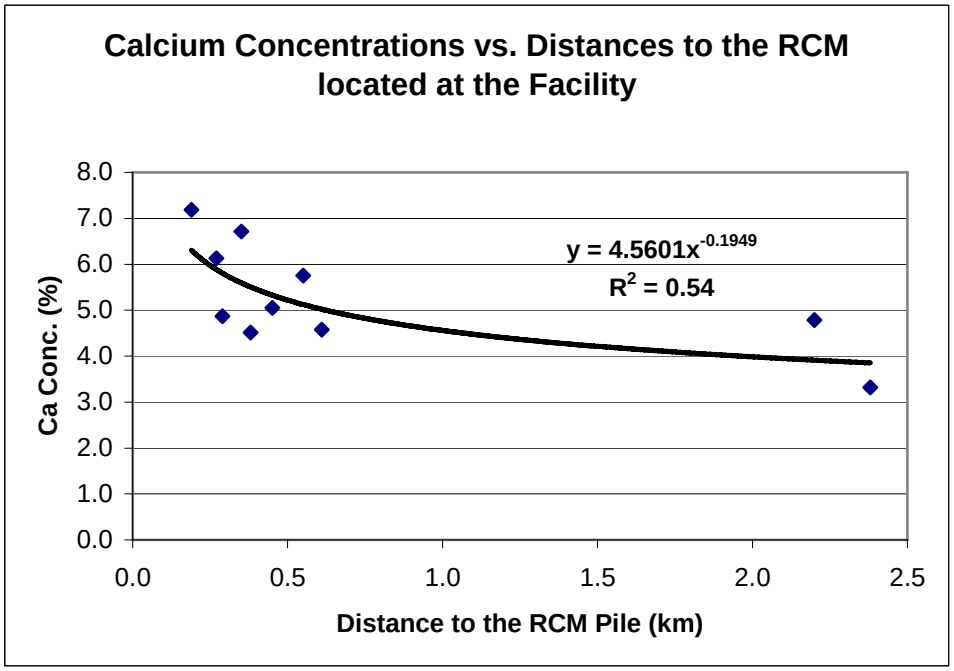

(a)

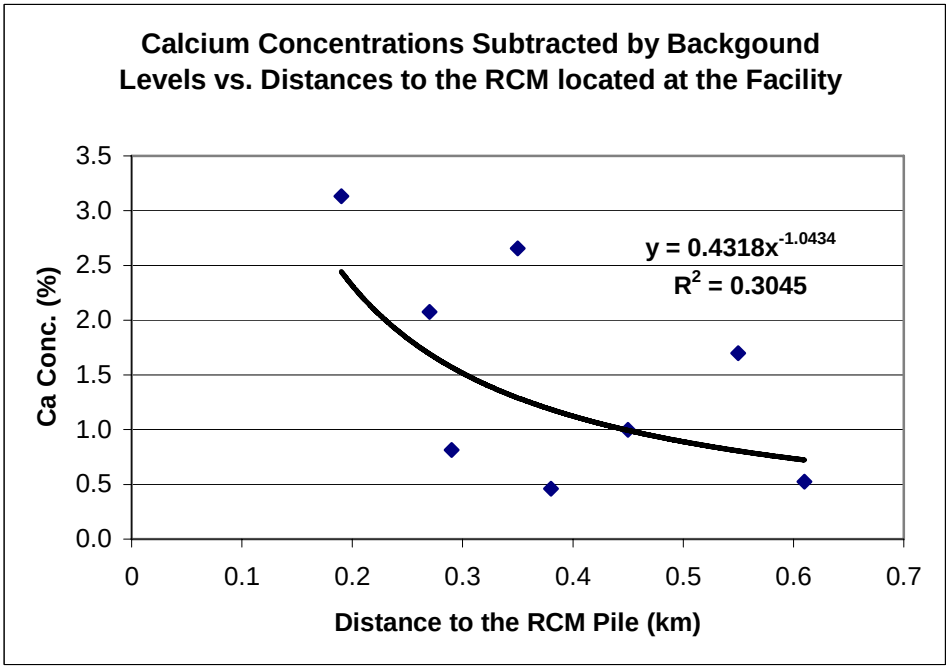

(b)

Figure 6. The scatter-plot of the %Ca concentrations obtained from the deposited filters (a) and the %Ca concentrations subtracted by the background level (b) vs. the distances (km) from each sampling site to the RCM pile located at the cement facility.

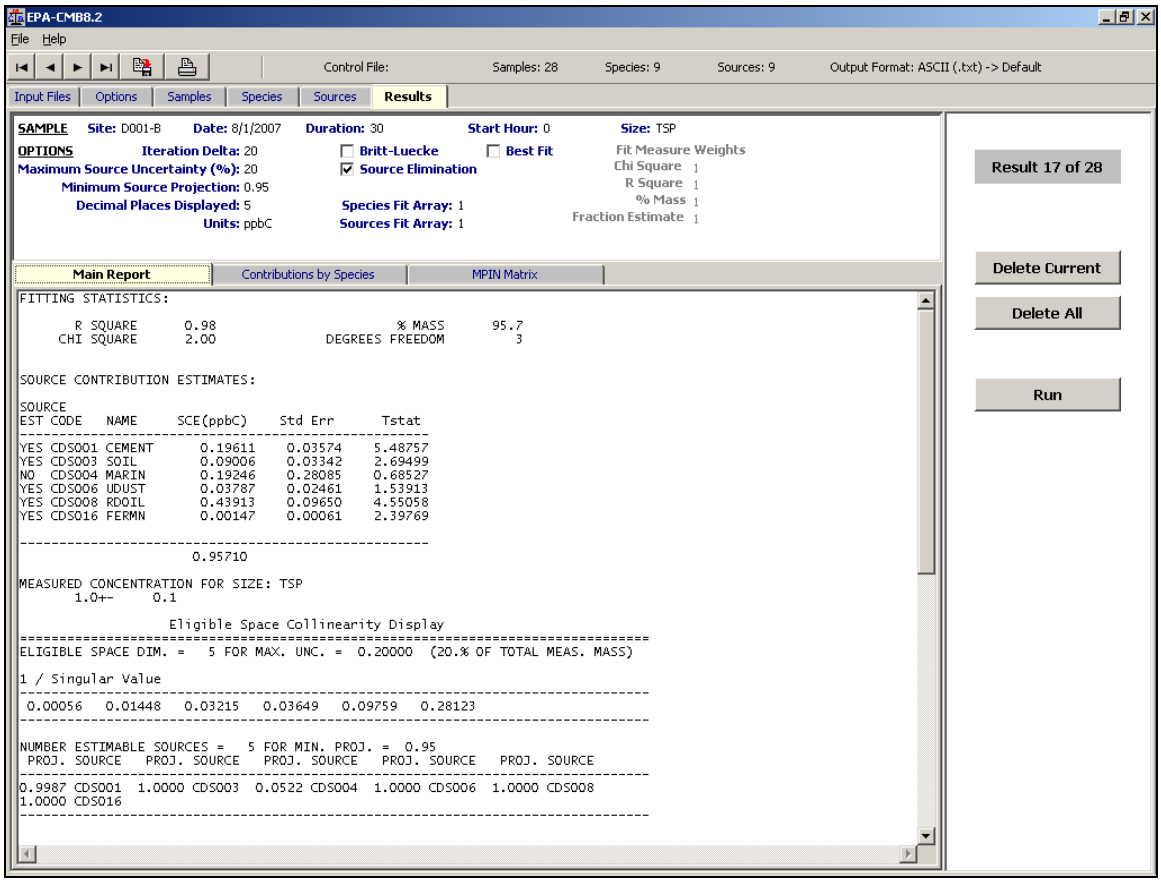

Figure 7. The screenshot of a CMB running for a dust deposition sample (D001-B).

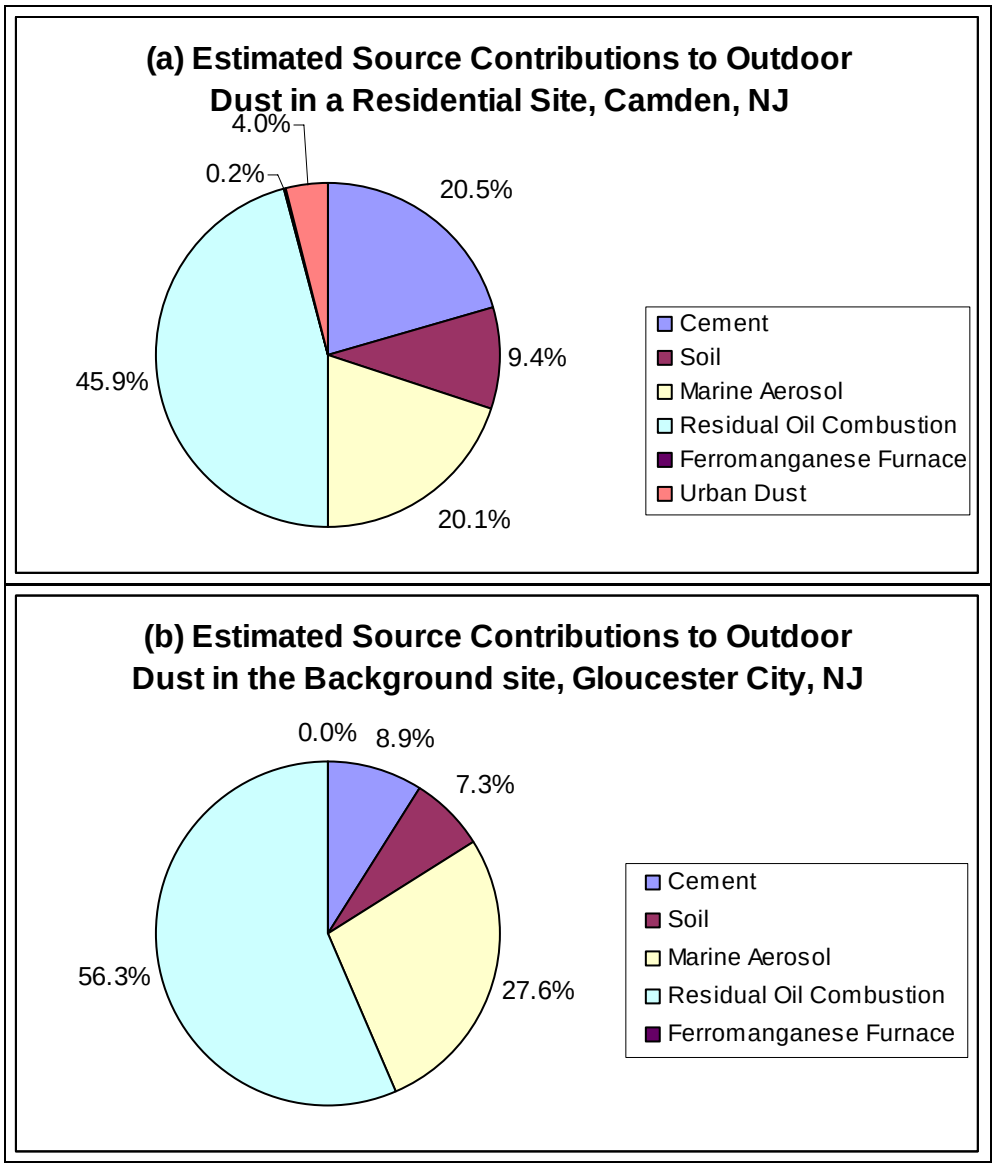

Figure 8. The pie-chart for estimation of source contributions to outdoor dust in a residential area near the cement facility (a) and in Gloucester City Park distant over 2 km upwind of the cement facility (b).

APPENDIX I.

Estimation of Deposition Flux and Contributions to Outdoor Dust around the Cement Facility in WFS

Please note: all calculations and estimates based upon the modeling results are subject to errors, and probably overestimations because: 1. The emission estimates are considered constant from day to day, and 2. Some sources are considered as worst case scenarios

1. ISCST3 modeled 24-hour TSP concentrations (μg/m^3) at the radial distances with individual sources at the cement facility.

To estimate the contributions of the site and stack emissions to outdoor dust surrounding the cement facility, sources for ALL and EP3 highlighted in Table 12 were selected representing the overall site emissions and individual stack emissions, respectively, in this estimation.

Table 12. 24-hour TSP modeling concentrations (μg/m^3) conducted by NJDEP at downwind distances of 200, 500, and 800 m, from the cement facility with each source emissions.

SOURCE	DESCRIPTION	200m	500m	800m
ALL		56.17	26.95	16.7
SJPCCON1	South Jersey Port Corporation Pier 1A	3.65	3.58	1.91
SJPCCON2	South Jersey Port Corporation Crane Conveyor	2.72	0.83	0.55
EP2	PT15 - Roller mill recirculation dust filter	3.2	1.02	0.53
EP3	PT11 - Roller mill vent stack	6.08	4.5	3.59
EP10	PT19 - Ground GBFS transport bucket elevator	1.06	0.59	0.33
EP11	Product dust filter #2	0.67	0.46	0.32
EP12	Product dust filter #3	0.64	0.44	0.31
EP14	Bulk loader dust filter #1	2.32	0.71	0.42
EP15	Bulk loader dust filter #2	1.42	0.64	0.42
EP16	PT26 - Transport to bulk loader dust filter	1.24	1.13	0.42
EP17	PT27 - Bulk loader dust filter #3	1.31	0.75	0.46
EP18	PT28 - Bulk loader dust filter #4	2.03	0.75	0.44
EP19	Bulk loader dust filter #1	1.36	0.33	0.21
EP20	PT20 - Product dust filter	1.13	0.6	0.38
EP21	PT30 - Product distribution dust filter (Barge)	4.99	2.91	1.92
GENERATOR	PT22 - Stack generator	0.82	0.41	0.22
RADIAL_S	Radial stacker	3.8	1.92	0.75
FEEDCONV	Feed Conveyor	1	0.1	0.06
CONV2	Conveyor 2	0.58	0.11	0.05
CONV3	Conveyor 3	0.21	0.08	0.04
CONV4	Conveyor 4	0.01	0.0075	0.0036
CONV5	Conveyor 5	0.04	0.01	0.006
PRODTRUK	Product trucks	26.5	7.69	4.09
EASTPILE	East pile	5.16	0.57	0.27
UPILE	Horseshoe-shaped pile	1.77	0.7	0.47
NEW	All new sources since 2000	15.04	7.47	5.38

2. Deposition flux estimated from field sampling data collected by EOHSI

From two field sampling campaigns in WFS, deposition flux was directly calculated at each sampling location and provided in Table 13. The deposition flux ranged from 24 to 83 mg/m^2-day within the radial distances between 190 and 660 m.

Table 13. Deposition flux calculated through field sampling measurements.

1st Sampling (3 weeks)				2nd Sampling (1 month)			
Location	Distance (km)	Mass (mg)	Deposition Flux (mg/m^2-day)	Location	Distance (km)	Mass (mg)	Deposition flux (mg/m^2-day)
1	0.23	1.542	68	1	0.19	1.604	48
2	0.37	1.880	83	2	0.29	1.230	37
4	0.36	1.422	63	3	0.27	1.216	37
5	0.50	0.912	40	4	0.35	0.796	24
6	0.66	1.098	49	5	0.38	1.600	48
7	0.65	1.427	63	6	0.61	1.062	32
9	0.55	0.768	34	7	0.55	1.072	32
12	0.45	0.966	43	8	0.45	0.904	27
				9[a]	2.38	0.447	13
				10[a]	2.20	0.555	17

[a]The locations are background sites located upwind from the cement facility in Gloucester City Park.

3. Mass % calculated each particle range in deposition filters

Based on particle number counts for three deposition filters, we calculated the averaged number and mass percentages in each diameter range (Table 14). The deposition velocity calculated in the following section depends on the particle size; therefore, a mid point was obtained from each particle range and used for further calculations of deposition velocities.

Table 14. The particle size distribution (percent by count) for deposition filters and the corresponding mass percentages for each particle diameter.

Diameter Range (μm)	Particle Diameter[a] (μm)	D001-A	D003-B	D-005A	Averaged Number %	Averaged Mass %
0.5-1.0	0.75	36.5	4.4	26.8	22.6	0.4
1.0-2.5	1.75	51.6	79.6	58.4	63.2	13.3
2.5-5.0	3.75	8.3	15.9	10.7	11.6	24.0
5.0-7.5	6.25	1.5	0.0	2.1	1.2	11.5
7.5-10.0	8.75	0.7	0.1	0.7	0.5	13.1
>10.0	10.0	1.5	0.0	1.4	1.0	37.8

[a]The particle diameter was obtained as a middle point of two values and used as the uniform particle diameter in each range for further calculations.

4. Deposition flux estimated from TSP concentrations predicted by ISCST3 model

The dry deposition flux (F) is directly proportional to the airborne concentrations (C) and a size-dependent deposition velocity (V_d) at some reference height (Z_r) above the surface (Lim et al., 2006).

$$F = C \cdot V_d \tag{4}$$

The size-dependent deposition velocity (V_d) can be calculated with a gravitational settling velocity (V_g) in the atmosphere.

$$V_d = \frac{1}{r_a + r_b + r_a \cdot r_b \cdot V_g} + V_g \tag{5}$$

where, r_a is the resistance due to turbulent transport through the overlying atmosphere to the molecular sub-layer, and
r_b is the resistance of the molecular scale diffusive transport at the boundary.

The aerodynamic resistance (r_a) can be obtained by

$$\begin{aligned} r_a &= \frac{0.74}{C_d v_r} \\ C_d &= \left[\frac{k}{\ln(Z_r / Z_0)} \right] \end{aligned} \tag{6}$$

where, v_r is the velocity at height Z_r (≈ 14.076 km/hr, averaged by main wind direction between 190 and 260 degrees from the normalized wind frequency data for the period of 1991 ~ 1995 at the Philadelphia Int'l Airport),
C_d is a drag force coefficient,
k is the Von Karman constant (0.41),
Z_r is the reference height (≈ 2.1336 m, the weather data has been monitored at 7 ft above sea level in Philadelphia Int'l Airport), and
Z_0 is the aerodynamic surface roughness height (assumed 1 m here).

The resistance (r_b) can be obtained by

$$\begin{aligned} r_b &= \frac{2 \cdot Sc^{2/3}}{k \cdot C_d^{1/2} \cdot v_r} \\ Sc &= \frac{\mu}{\rho_a \cdot D_p} \\ D_p &= \frac{k_B \cdot T}{6\pi \cdot d_p \cdot \mu} \end{aligned} \tag{7}$$

where, Sc is the Schmidt number representing the transportation of particles by Brownian diffusion,
μ is the dynamic viscosity of dry air at 293 K (1.81×10^{-5} N·sec/m^2),
ρ_a is the density of dry air at 293 K and 1 atm (1.2 kg/m^3),
D_p is the Brownian diffusion coefficient as a function of particle diameter d_p,
k_B is the Boltzman's constant (1.38×10^{-23} N·m/K), and

T is the absolute temperature (assumed 293 K here).

The gravitational settling velocity (V_g) can be obtained by

$$V_g = \frac{(\rho_p - \rho_a) \cdot g \cdot d_p^{\,2} \cdot C_c}{18\mu} \quad (8)$$

where, ρ_p is the density of particles (assumed 1,800 kg/m^3),

g is the gravitation acceleration (9.8 m/sec^2), and

C_c is the Cunningham slip correction factor ranging from 1.21075~1.015 in the calculation. The factor was directly obtained from a Table (Hinds, 1999) or interpolated between two closest values, if not in the Table.

Using the above equations, deposition fluxes (mg/m^2-day) were back-calculated from the model-predicted TSP concentrations at radial distances from the facility with 200 m, 500 m, and 800 m. Two cases of deposition fluxes, representing 24-hour TSP concentrations by the overall site emissions and the individual stack emission of EP3, were provided in Table 15. The deposition flux within the radial distance of 100 m was not included in the estimation, because the deposition of dusts within that range may be affected by air movements such as eddies and turbulences, and cannot be reliably estimated by the model. The deposition flux at each particle size should be corrected by corresponding mass percentages in Table 14. The correction was conducted by multiplying the deposition flux with corresponding particle mass percentage and the corrected deposition fluxes were provided in Table 15. The deposition fluxes for site emissions and stack emissions were estimated ranging from 4.46 ~ 15.01 mg/m^2-day and 0.96 ~ 1.62 mg/m^2-day, respectively, at the distances between 200 and 800 m.

Table 15. The deposition fluxes calculated from equation 1 and the deposition fluxes corrected by particle mass percentage for each size range.

Particle Diameter (μm)	Deposition Flux (mg/m^2-day)			Corrected Deposition Flux[a] (mg/m^2-day)		
	200 m	500 m	800 m	200 m	500 m	800 m
0.75	0.2 (0.0)	0.1 (0.0)	0.1 (0.0)	0.00 (0.00)	0.00 (0.00)	0.00 (0.00)
1.75	0.9 (0.1)	0.4 (0.1)	0.3 (0.1)	0.12 (0.01)	0.06 (0.01)	0.03 (0.01)
3.75	3.9 (0.4)	1.9 (0.3)	1.2 (0.2)	0.93 (0.10)	0.45 (0.07)	0.28 (0.06)
6.75	10.5 (1.1)	5.0 (0.8)	3.1 (0.7)	1.21 (0.13)	0.58 (0.10)	0.36 (0.08)
8.75	20.5 (2.2)	9.8 (1.6)	6.1 (1.3)	2.68 (0.29)	1.29 (0.21)	0.80 (0.17)
10.0	26.7 (2.9)	12.8 (2.1)	7.9 (1.7)	10.08 (1.09)	4.84 (0.81)	3.00 (0.64)
Total				15.01 (1.62)	7.20 (1.20)	4.46 (0.96)

Note: Value in parenthesis indicates the deposition fluxes calculated by TSP concentration for the single stack emission of EP3.

[a]The deposition fluxes were corrected by the mass percentage for each particle range.

5. Contribution of overall site and individual stack emissions to outdoor dust downwind the cement facility in WFS

The site and stack emissions contribution to the outdoor dust downwind the cement facility in WFS was estimated by equation (9), and the results are presented in Table 16. Since no background data available in the first field study (samples were lost during sampling period), estimation was conducted only for the results collected from the second sampling conducted in the study.

$$\text{Site/Stack Emissions Contribution (\%)} = \frac{D_c}{D_m} \times 100 \qquad (9)$$

where, D_c is a deposition flux calculated from the ISCST3 model for the radial distances of 200, 500 and 800 m, and

D_m is a deposition flux obtained from a regression equation (see Figure 9) based on field measurements in WFS at the radial distances of 200, 500, and 800 m.

The estimated contributions of the entire site emissions to outdoor settled dust using the ISCST3 model were 33.7%, 24.1%, and 18.3% for sampling distances of 200 m, 500 m, and 800 m, respectively. The contributions by a single stack emission in the facility were only a small fraction of the total emissions of the facility, ranging from 3.6% to 4.9% for the same sampling locations. These results are reasonable since dust deposition is not expected to be significant in short distances given the height of the stack.

The results estimated by the ISCST3 model were compared to the CMB modeling results and those estimated by the Ca concentrations. As shown in Table 16, the estimated contribution of cement pile at the cement facility to outdoor dust in WFS ranged from 5.6% to 21.2% based on the CMB model and from 2.4% and 8.1% based on the regression analysis using the Ca concentrations of the deposition samples. The contributions from all site emissions predicted by ISCST3 model, including operations of the plant, transportation of RCM by trucks, and stack emissions at the facility, were higher than the CMB results as well as Ca-regression estimates. The higher contributions estimated for the total site emissions by the ISCST3 were reasonable, because in a number of cases these were worst case scenario estimates of emissions and the source strengths were of each stack and operations were considered constant each day.

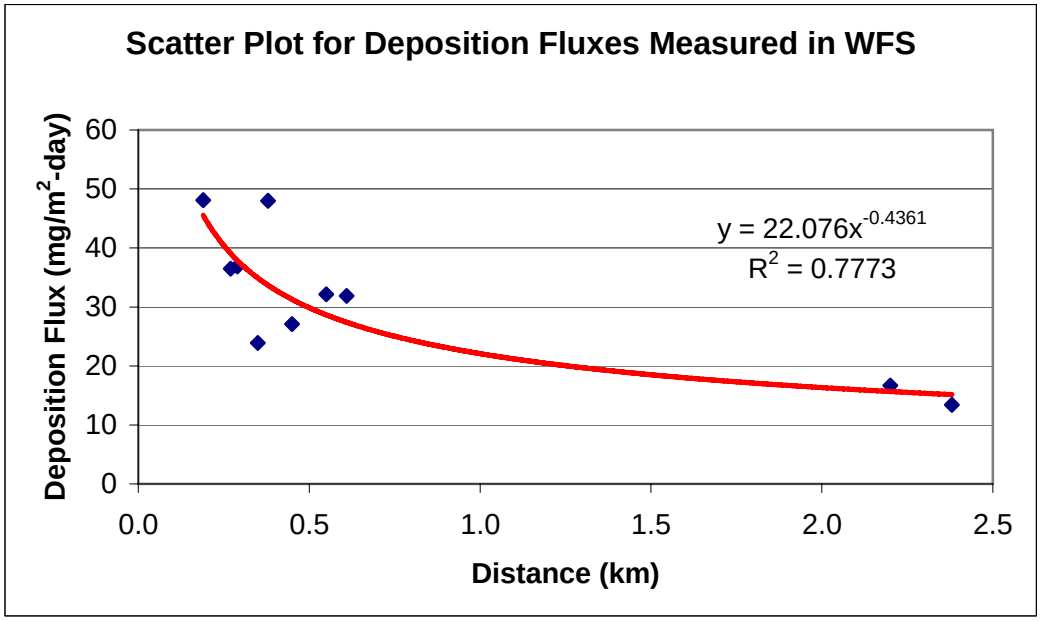

Figure 9. The scatter plot and its regression equation for deposition fluxes measured along the cement pile at the facility in WFS from measurements made by EOHSI.

Table 16. The contribution of cement pile (left) estimated by CMB and the site/stack emissions (right) estimates by ISCST3 model to the total outdoor dust around the cement facility in WFS.

L.	Distance (km)	Deposition Flux (mg/m^2-day)	Cement Pile Contribution[a]		Distance 0.2 km	Distance 0.5 km	Distance 0.8 km
1	0.19	48	21.2%	Calculated Deposition Flux (D_c) (mg/m^2-day)	15.0 (1.62)	7.20 (1.20)	4.46 (0.96)
2	0.29	37	13.9%				
3	0.27	37	17.0%				
4	0.35	24	12.4%				
5	0.38	48	14.0%	Measured Deposition Flux (D_m) (mg/m^2-day)[b]	44.5	29.9	24.3
6	0.61	32	9.0%				
7	0.55	32	5.6%				
8	0.45	27	10.9%				
9[c]	2.38	13	8.9%	Site/Stack Emissions Contribution (%)[d]	33.7 (3.6)	24.1 (4.0)	18.3 (3.9)
10[c]	2.20	17	8.9%				

Note: Value in parenthesis indicates the deposition fluxes calculated by TSP concentration for the single stack emission of EP3.

[a]The contribution to outdoor dust was estimated by CMB model from the cement pile at the facility in WFS.

[b]The deposition flux (D_m) was obtained from a regression equation ($Y=22.076X^{-0.4361}$) at each distance.

[c]The locations are background sites located upwind from the cement facility in Gloucester City Park.

[d]The contribution to outdoor dust was estimated from the site/stack emissions in the cement facility.

APPENDIX II. MVA report for D-001A and D-005A.

Revised Report of Results: MVAS948

Microscopical Analysis of Particles on Filters
Emissions Study

Prepared for:

EOHSI
170 Frelinghuysen Road
Piscataway, NJ 08854

Respectfully Submitted by:

Bryan Bandli
Senior Research Scientist

James R. Millette, Ph.D.
Executive Director

MVA Scientific Consultants
3300 Breckinridge Boulevard
Suite 400
Duluth, GA 30096

Supercedes Report Dated 04 February 2008

07 February 2008

MVA SCIENTIFIC CONSULTANTS

6948report020408_rev1_020708

Revised Report of Results: MVA6948

Microscopical Analysis of Particles on Filters
Emissions Study

INTRODUCTION

This revised report includes the results of scanning electron microscopy (SEM) particle elemental analysis and polarized light microscopy (PLM) analysis of two soil samples delivered on quartz fiber filters to MVA Scientific Consultants on 30 November 2007. Upon receipt the samples were assigned the following identification numbers:

MVA ID	EOHSI ID
S1699	D001-A
S1700	D005-A

MVA was asked to provide information about the composition and morphology of the samples. The work was done as part of the EOHSI project: "Contribution of Particle Emissions from a Cement Facility to Outdoor Dust in Surrounding Community."

Analyses were performed at MVA Scientific Consultants during the period 12 December through 30 January 2008.

METHODS

The particulate on the filter samples was prepared by lifting the particles off the surface of the filters using glycerol. The glycerol was diluted in deionized water and filtered onto 0.4μm diameter pore size polycarbonate membrane filters. The analyses were performed using a JEOL Model JSM-6500F field emission scanning electron microscope operating in automated mode under the control of a Thermo Noran System SIX x-ray analysis system. Elemental composition were collected using x-ray analysis for 21 elements: Na, Mg, Al, Si, P, S, Cl, K, Ca, Ti, V, Cr, Mn, Fe, Ni, Cu, Zn, Zr, Cd, Ba and Pb. Data were obtained for a minimum of 1000 particles. The data are tabulated in two ways: by number of particles that contain an element in significant amounts and by element groupings that show predominate elemental associations in the particles.

To aid with the interpretation of the data, additional analysis by polarized light microscopy was also performed on each sample. The methodology used in this analysis is similar to what was previously used for a sample analyzed by MVA in February/March 2007 (see report issued 01 March 2007). The samples were examined under an Olympus SZ-40 stereomicroscope at magnifications from 7 to 40X. Particles from the sample were mounted in 1.55 RI Cargille liquid for analysis by polarized light microscopy using an Olympus BH-2 polarized light microscope with a magnification range from 100 to 1000X.

Table 1. Occurrence of Particles by Element*

Client ID	D001-A		D005-A	
MVA ID	S1699		S1700	
	#	%	#	%
Na	0	0.0	0	0.0
Mg	1	0.1	8	0.6
Al	5	0.5	10	0.8
Si	823	87.9	1059	79.7
P	0	0.0	0	0.0
S	2	0.2	4	0.3
Cl	0	0.0	0	0.0
K	0	0.0	0	0.0
Ca	24	2.6	74	5.6
Ti	6	0.6	9	0.7
V	0	0.0	0	0.0
Cr	0	0.0	0	0.0
Mn	0	0.0	1	0.1
Fe	64	6.8	149	11.2
Ni	0	0.0	0	0.0
Cu	1	0.1	0	0.0
Zn	3	0.3	2	0.2
Zr	1	0.1	3	0.2
Cd	0	0.0	0	0.0
Ba	0	0.0	0	0.0
Pb	6	0.6	9	0.7

*Presence of an element was based on over 40 weight % of the particle based on the 21 elements determined by x-ray analysis.

Table 2. Groupings of Elements in Particles

Client ID	D001-A		D005-A	
MVA ID	S1699		S1700	
Type	#	%	#	%
Al-rich	3	0.2	6	0.3
Si-rich	528	43.8	679	38.0
S-rich	1	0.1	1	0.1
Ca-rich	7	0.6	30	1.7
Ti-rich	4	0.3	7	0.4
Mn-rich	0	0.0	1	0.1
Fe-rich	50	4.1	111	6.2
Cu-rich	1	0.1	0	0.0
Zn-rich	3	0.2	2	0.1
Zr-rich	1	0.1	1	0.1
Pb-rich	0	0.0	2	0.1
Ca+Fe	2	0.2	1	0.1
Ca-rich Silicate	23	1.9	48	2.7
KAlSi	40	3.3	76	4.3
MgAl	23	1.9	61	3.4
SiAlFe	194	16.1	394	22.1
Mixed Silicate	257	21.3	225	12.6
Ca+Mg	16	1.3	39	2.2
Mixed Fe	14	1.2	46	2.6
Unclassified	38	3.2	56	3.1

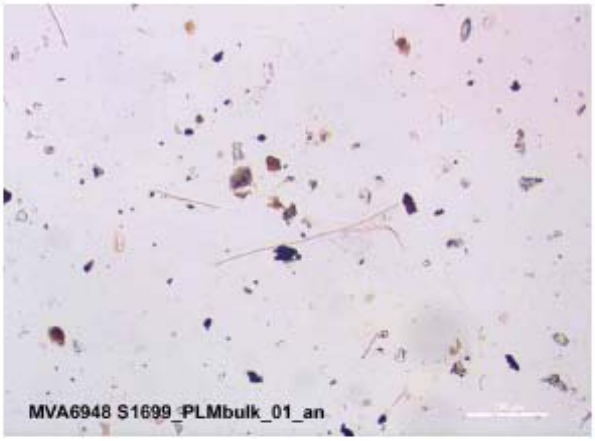

Figure 1. Particles in Sample S1699, transmitted light.

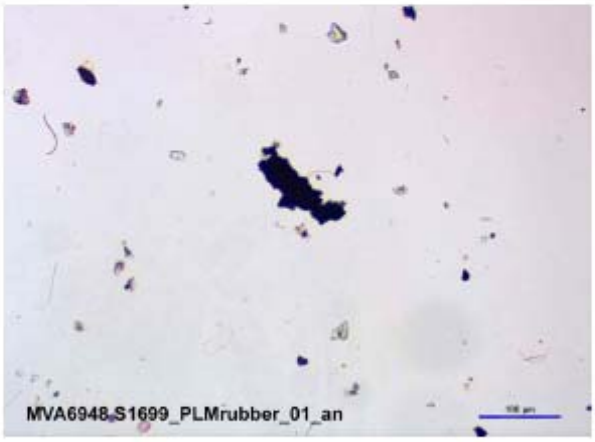

Figure 2. Rubber particles in Sample S1699, reflected light.

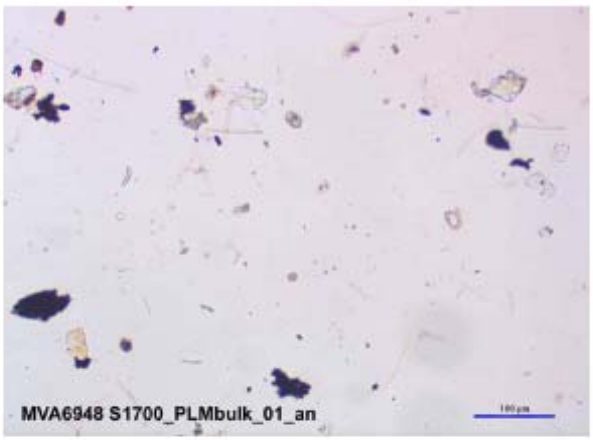

Figure 3. Particles in Sample S1700, transmitted light.

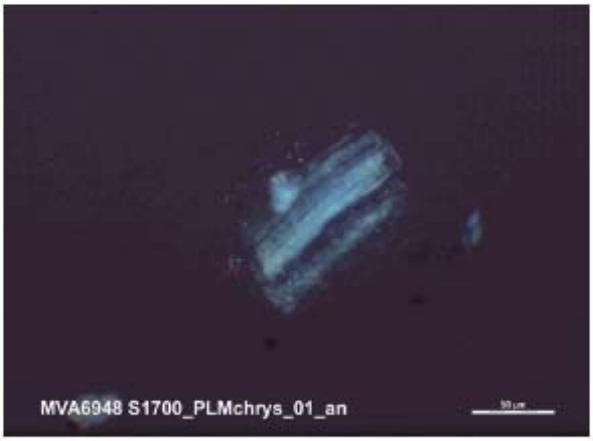

Figure 4. Chrysotile bundle in Sample S1700, transmitted cross-polarized light.

Table 1. Particle Size Distributions in Terms of Number of Particles in Size Ranges

	S1699 D001-A	S1699 D001-A	S1700 D005-A	S1700 D005-A
Diameter (µm)	Number	Percent	Number	Percent
0.5-1.0	440	36.5%	536	26.8%
1.0-2.5	622	51.6%	1167	58.4%
2.5-5.0	100	8.3%	214	10.7%
5.0-7.5	18	1.5%	42	2.1%
7.5-10.0	8	0.7%	14	0.7%
>10.0	18	1.5%	27	1.4%
Total Particles	1206		2000	

6948Lt-Suppl-sizedata022508

APPENDIX III. MVA report for D-003B, D-018C and D-017D.

Report of Results: MVA6948

Microscopical Analysis of Particles on Filters
Emissions Study - D003-B, D018-C, D017-D

Prepared for:

EOHSI
170 Frelinghuysen Road
Piscataway, NJ 08854

Respectfully Submitted by: _____

James R. Millette, Ph.D.
Executive Director

MVA Scientific Consultants
3300 Breckinridge Boulevard
Suite 400
Duluth, GA 30096

29 February 2008

6948report022908

Report of Results: MVA6948

Microscopical Analysis of Particles on Filters
Emissions Study - D003-B, D018-C, D017-D

INTRODUCTION

This report includes the results of scanning electron microscopy (SEM) particle elemental analysis and polarized light microscopy (PLM) analysis of three samples delivered on quartz fiber filters to MVA Scientific Consultants on 21 December 2007. Upon receipt the samples were assigned the following identification numbers:

MVA ID	EOHSI ID
S1857	D003-B
S1858	D018-C
S1859	D017-D

MVA was asked to provide information about the particle size, composition and morphology of the samples. The work was done as part of the EOHSI project: "Contribution of Particle Emissions from a Cement Facility to Outdoor Dust in Surrounding Community."

Analyses were performed at MVA Scientific Consultants during the period 29 January through 22 February 2008.

METHODS

The particulate on the filter samples was prepared by lifting the particles off the surface of the filters using glycerol. The glycerol was diluted in deionized water and filtered onto 0.4μm diameter pore size polycarbonate membrane filters. The analyses were performed using a JEOL Model JSM-6500F field emission scanning electron microscope operating in automated mode under the control of a Thermo Noran System SIX x-ray analysis system. Elemental compositions were collected using x-ray analysis for 21 elements: Na, Mg, Al, Si, P, Cl, K, Ca, Ti, V, Cr, Mn, Fe, Ni, Co, Cu, Zn, Zr, Cd, Ba, and Pb. The data are tabulated in three ways: by particle size, by number of particles that contain an element in significant amounts and by element groupings that show predominate elemental associations in the particles.

To aid with the interpretation of the data, additional analysis by polarized light microscopy was also performed on each sample. The methodology used in this analysis is similar to what was previously used for a sample analyzed by MVA in February/March 2007 (see report issued 01 March 2007). Distilled, filtered water was used to wash the particles from the glass fiber filters. The particles were examined under an Olympus SZ-40 stereomicroscope at magnifications from 7 to 40X. Particles from the sample were mounted in 1.55 RI Cargille liquid for analysis by polarized light

microscopy using an Olympus BH-2 polarized light microscope with a magnification range from 100 to 1000X.

RESULTS

Particle size data and elemental data determined by SEM-EDS for all three samples are shown in Tables 1, 2, and 3. Representative images of the particles in the samples are shown in Figures 1, 2, and 3. The PLM particle type analysis is given below. The percent estimates are given in terms of % volume of a particle type.

Sample S1857 (D003-B). The mean particle diameter as determined by SEM is 1.6 μm. The maximum is 10.9 μm and the minimum is 0.6 μm. PLM analysis shows that the sample is composed of major components: soil minerals including quartz, carbonate and mica (30-40%), plant fragments (10-20%), and rubber particles (10-20%); minor components: fungal material (5-10%), soot (5-10%), cotton fibers (1-5%), and rust/metal flakes (1-5%); and trace (less than 1%) components: pollen grains, synthetic fibers, glass fibers (excluding the glass fibers from the filter), construction debris, and insect parts. No cement clinker particles were detected. Calcium-containing particles and calcium-silicate particles, both consistent with cement products as well as some types of soil minerals, were minor components (less than 10%) of the particulate population.

Sample S1858 (D018-C). The mean particle diameter as determined by SEM is 1.6 μm. The maximum is 31.4 μm and the minimum is 0.5 μm. PLM analysis shows that the sample is composed of major components: soil minerals including quartz, carbonate and mica (30-40%) and rubber particles (10-20%); minor components: fungal material (5-10%), soot (5-10%), plant fragments (5-10%), cotton fibers (5-10%), and rust/metal flakes (1-5%); and trace (less than 1%) components: pollen grains, synthetic fibers, construction debris, and starch. No cement clinker particles were detected. Calcium-containing particles and calcium-silicate particles, both consistent with cement products as well as some types of soil minerals, were minor components (less than 10%) of the particulate population.

Sample S1859 (D017-D). The mean particle diameter as determined by SEM is 2.2 μm. The maximum is 32.3 μm and the minimum is 0.5 μm. PLM analysis shows that the sample is composed of major components: soil minerals including quartz, carbonate, feldspar and mica (40-60%) and soot (10-15%); minor components: fungal material (5-10%), plant fragments (5-10%), cotton fibers (5-10%), rust/metal flakes (1-5%) and rubber particles (5-10%); and trace (less than 1%) components: pollen grains, paint, and insect parts. No cement clinker particles were detected. Calcium-containing particles and calcium-silicate particles, both consistent with cement products as well as some types of soil minerals, were minor components (less than 10%) of the particulate population.

DISCUSSION

The elemental data in Table 2 shows that the samples are generally similar to one another in terms of chemical composition.

Table 3 shows that all three samples contain a significant quantity of silicon-rich particles. However, it should be noted that the quartz fiber filters used to collect the sample did release some quartz fibers (Si-fibers) into the particulate prepared for analysis. Although considerable effort was made to remove the data generated by the Si-fiber particles from the dataset, some may have been included with the data shown in Tables 2 and 3.

Table 1. Particle Size Distributions in Terms of Number of Particles in Size Ranges

	S1857	S1857	S1858	S1858	S1859	S1859
Diameter (μm)	Number	Percent	Number	Percent	Number	Percent
0.5-1.0	39	4.4%	227	23.9%	219	24.3%
1.0-2.5	708	79.6%	607	64.0%	486	53.9%
2.5-5.0	141	15.9%	142	14.2%	134	14.9%
5.0-7.5	0	0.0%	16	1.7%	21	2.3%
7.5-10.0	1	0.1%	4	0.4%	16	1.8%
>10.0	0	0.0%	3	0.3%	26	2.9%
Total Particles	889		999		902	

Table 2. Occurrence of Particles by Element*

	S1857	S1857	S1858	S1858	S1859	S1859
Element	Number	Percent	Number	Percent	Number	Percent
Na	0	0.0%	0	0.0%	0	0.0%
Mg	0	0.0%	0	0.0%	0	0.0%
Al	3	0.3%	0	0.0%	5	0.6%
Si	500	56.2%	580	58.1%	539	59.8%
P	0	0.0%	0	0.0%	0	0.0%
Cl	0	0.0%	0	0.0%	0	0.0%
K	0	0.0%	0	0.0%	1	0.1%
Ca	25	2.8%	69	6.9%	33	3.7%
Ti	14	1.6%	2	0.2%	7	0.8%
V	0	0.0%	0	0.0%	0	0.0%
Cr	2	0.2%	0	0.0%	0	0.0%
Mn	1	0.1%	0	0.0%	0	0.0%
Fe	32	3.6%	72	7.2%	61	6.8%
Co	0	0.0%	0	0.0%	0	0.0%
Ni	0	0.0%	0	0.0%	0	0.0%
Cu	0	0.0%	0	0.0%	0	0.0%
Zn	3	0.3%	0	0.0%	0	0.0%
Zr	2	0.2%	0	0.0%	0	0.0%
Cd	0	0.0%	0	0.0%	0	0.0%
Ba	1	0.1%	0	0.0%	0	0.0%
Pb	1	0.1%	0	0.0%	0	0.0%

*Presence of an element was based on over 40 weight % of the particle based on the 21 elements determined by x-ray analysis. The sums of the percents do not total 100% because some particles contain a mixture of elements where no element is over 40%.

Table 3. Groupings of Elements in Particles

	S1857	S1857	S1858	S1858	S1859	S1859
Particle Type	#	%	#	%	#	%
Al-rich	0	0.0%	3	0.3%	1	0.1%
Si-rich	443	49.8%	231	23.1%	346	38.4%
S-Rich	0	0.0%	4	0.4%	3	0.3%
Ca-rich	0	0.0%	21	2.1%	20	2.2%
Ti-rich	2	0.2%	11	1.1%	4	0.4%
Mn-rich	0	0.0%	1	0.1%	0	0.0%
Fe-rich	72	8.1%	0	0.0%	46	5.1%
Cu-rich	0	0.0%	3	0.3%	0	0.0%
Zn-rich	0	0.0%	2	0.2%	0	0.0%
Zr-rich	0	0.0%	2	0.2%	1	0.1%
Pb-rich	0	0.0%	0	0.0%	0	0.0%
Ca+Fe	0	0.0%	0	0.0%	1	0.1%
Ca-richSilicate	69	7.8%	4	0.4%	31	3.4%
KAlSi	13	1.5%	78	7.8%	75	8.3%
MgAl	0	0.0%	1	0.1%	1	0.1%
SiAlFe	12	1.3%	81	8.1%	0	0.0%
MixedSilicate	276	31.0%	454	45.4%	320	35.5%
Ca+Mg	0	0.0%	5	0.5%	5	0.6%
MixedFe	0	0.0%	47	4.7%	18	2.0%
Unclassified	2	0.2%	51	5.1%	30	3.3%
Total	889		999		902	

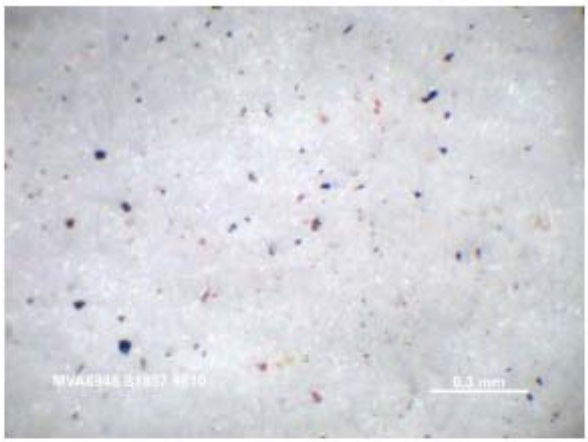

Figure 1. Particles on filter Sample S1857, reflected light.

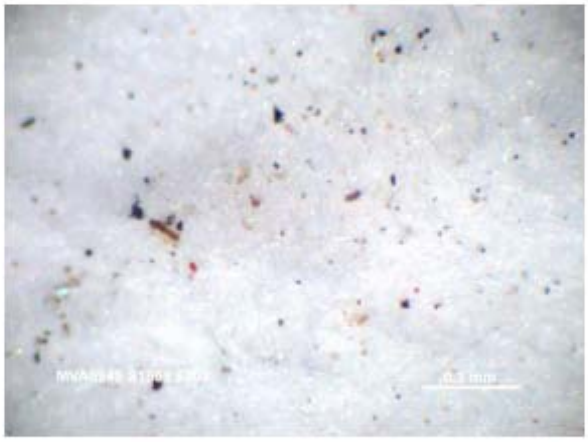

Figure 2. Rubber particles on filter Sample S1858, reflected light.

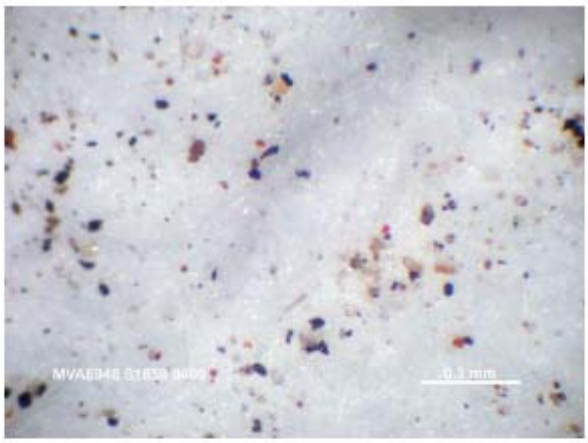

Figure 3. Particles on filter Sample S1859, reflected light.

APPENDIX IV. MVA report for RCM <38µm.

Report of Results: MVA6948

Microscopical Analysis of Particles
Emissions Study – RCM1<38um

Prepared for:

EOHSI
170 Frelinghuysen Road
Piscataway, NJ 08854

Respectfully Submitted by: _____

James R. Millette, Ph.D.
Executive Director

MVA Scientific Consultants
3300 Breckinridge Boulevard
Suite 400
Duluth, GA 30096

11 March 2008

6948report031108

Report of Results: MVA6948

Microscopical Analysis of Particles
Emissions Study – RCM1<38um

INTRODUCTION

This report includes the results of scanning electron microscopy (SEM) particle sizing, elemental analysis and polarized light microscopy (PLM) analysis of one sample delivered as a powder to MVA Scientific Consultants on 06 March 2008. The sample was identified as a raw cement material sample collected from a cement facility in Camden, New Jersey. Upon receipt the sample was assigned the following identification number:

MVA ID	EOHSI ID
T0507	RCM<38um

MVA was asked to provide information about the particle size, composition and morphology of the sample. The work was done as part of the EOHSI project: "Contribution of Particle Emissions from a Cement Facility to Outdoor Dust in Surrounding Community."

Analyses were performed at MVA Scientific Consultants during the period 06 March through 07 March 2008.

METHODS

The particulate was prepared by suspending a portion in isopropanol and placing a 10 micro-liter drop on a polycarbonate membrane filter that was on a sample stub. The analyses were performed using a JEOL Model JSM-6500F field emission scanning electron microscope (SEM) operating in automated mode under the control of a Thermo Noran System SIX x-ray analysis system. Elemental compositions were collected using x-ray analysis for 22 elements: Na, Mg, Al, Si, P, S, Cl, K, Ca, Ti, V, Cr, Mn, Fe, Ni, Cu, Zn, Zr, Cd, Sn, Ba, and Pb. The data are tabulated in three ways: by particle size, by number of particles that contain an element in significant amounts and by element groupings that show predominant elemental associations in the particles.

To aid with the interpretation of the data, additional analysis by polarized light microscopy was also performed on each sample. The methodology used in this analysis is similar to what was previously used for a sample analyzed by MVA in February/March 2007 (see report issued 01 March 2007). The particles were examined under an Olympus SZ-40 stereomicroscope at magnifications from 7 to 40X. Particles from the sample were mounted in 1.550 RI Cargille liquid for analysis by polarized light microscopy using an Olympus BH-2 polarized light microscope with a magnification range from 100 to 1000X.

RESULTS

Particle size data and elemental data determined by SEM-EDS for the sample are shown in Tables 1, 2, and 3. Representative images of the particles in the sample are shown in Figures 1, 2, and 3. The PLM particle type analysis is given below. The percent estimates are given in terms of % volume of a particle type.

Sample T0507 (RCM<38um). The mean particle diameter as determined by SEM is 1.8 μm with a range of 0.5 to 30.2 μm. PLM analysis shows that the sample is composed of major components: calcium carbonate (80-85%) and isotropic particles with conchoidal fracture (15%); minor components: rust/metal flakes (1-3%); and trace (less than 1%) components: rubber and coal/coke particles. No cement clinker particles were detected. Calcium-containing particles and silicon-containing particles dominate the particle types in Sample T0507.

Table 1. Particle Size Distributions in Terms of Number of Particles in Size Ranges

	T0507	T0507
Diameter (μm)	Number	Percent
0.5-1.0	532	56.0%
1.0-2.5	289	30.4%
2.5-5.0	62	6.5%
5.0-7.5	23	2.4%
7.5-10.0	15	1.6%
>10.0	29	3.1%
Total Particles	950	

Table 2. Occurrence of Particles by Element*

	T0507	T0507
Element	Number	Percent
Na	0	0.0%
Mg	0	0.0%
Al	1	0.1%
Si	528	55.6%
P	0	0.0%
S	0	0.0%
Cl	0	0.0%
K	0	0.0%
Ca	214	22.5%
Ti	0	0.0%
V	0	0.0%
Cr	0	0.0%
Mn	0	0.0%
Fe	11	1.2%
Ni	0	0.0%
Cu	1	0.1%
Zn	0	0.0%
Zr	0	0.0%
Cd	0	0.0%
Sn	1	0.1%
Ba	3	0.3%
Pb	0	0.0%

*Presence of an element was based on over 40 weight % of the particle based on the 22 elements determined by x-ray analysis. The sums of the percents do not total 100% because some particles contain a mixture of elements where no element is over 40%.

Table 3. Groupings of Elements in Particles

	T0507	T0507
Particle Type	#	%
Al-rich	0	0.0%
Si-rich	66	6.9%
S-Rich	0	0.0%
Ca-rich	201	21.2%
Ti-rich	0	0.0%
Mn-rich	0	0.0%
Fe-rich	10	1.1%
Cu-rich	0	0.0%
Zn-rich	0	0.0%
Zr-rich	0	0.0%
Pb-rich	0	0.0%
Ca+Fe	0	0.0%
Ca-richSilicate	79	8.3%
KAlSi	0	0.0%
MgAl	0	0.0%
SiAlFe	1	0.1%
MixedSilicate	532	56.0%
Ca+Mg	0	0.0%
MixedFe	2	0.2%
Unclassified	59	6.2%
Total	950	

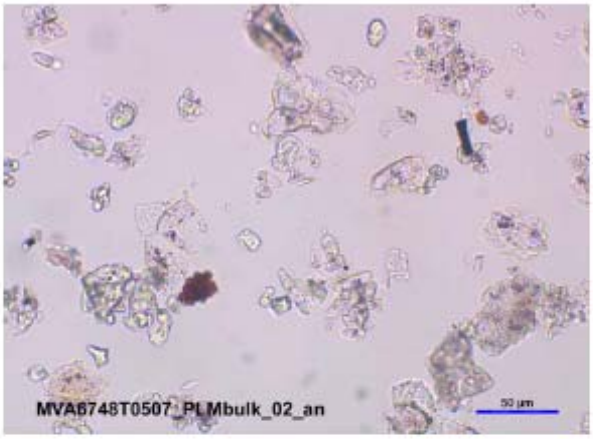

Figure 1. Particles in Sample T0507, transmitted light.

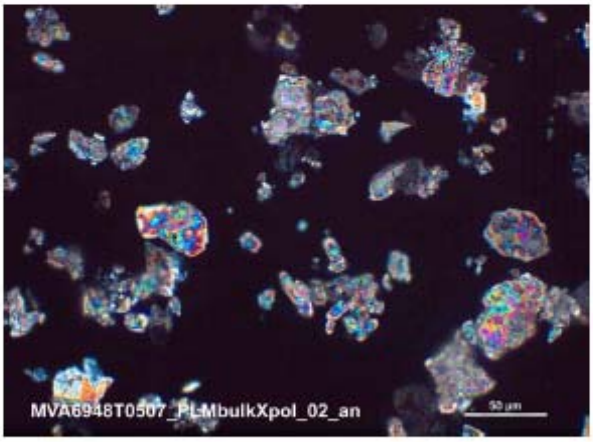

Figure 2. Particles in Sample T0507, crossed polars.

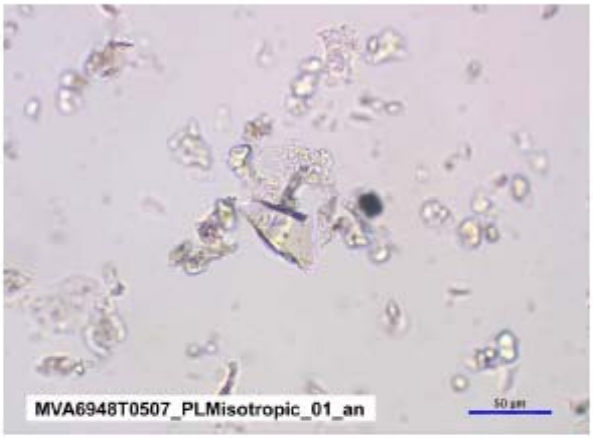

Figure 3. Isotropic particles in Sample T0507.